HAIT Journal of Science and Engineering, Volume 1, Issue 2, pp. 306-347

Light interaction with smectic A liquid crystals: nonlinear effects

Boris I. Lembrikov

Research Center for Quantum Communication Engineering
at Department of Communication Engineering,
Holon Academic Institute of Technology,
52 Golomb Str., Holon 58102, Israel
e-mail: borisle@hait.ac.il
Received 11 December 2003, revised 25 May 2004, accepted 1 June 2004

Abstract

The theory of non-linear optical effects and related electrodynamic and hydrodynamic effects in smectic A liquid crystals caused by a specific nonlinearity mechanism, the so-called second sound, is reviewed. We investigated the peculiarities of light self-focusing, self-trapping and nonlinear wave-mixing in smectic A liquid crystals. It is also shown that a light-induced high frequency longitudinal electric field and a hydrodynamic flow can be created. Nonlinear optical characteristics of smectic A liquid crystals are one or two orders of magnitude larger than similar quantities in isotropic organic liquids.

PACS: 42.70.Df, 61.30.Gd, 42.65.Es, 42.65.Sf, 42.65.Tg

1 Introduction

Liquid crystals (LC) possess unique physical properties intermediate between ordinary fluids and solids [1, 2]. There exist three types of liquid crystals: thermotropic, lyotropic and polymeric [1, 2]. In this work we consider only thermotropic LC which manifest the phase transitions related to their degree of ordering in a definite temperature range [1, 2]. Usually they consist of organic molecules elongated in one direction. Electrodynamics of

thermotropic LC has been recently reviewed in [3]. Thermotropic LC, in turn, are classified as follows [1, 2]. Nematic liquid crystals (NLC) are characterized by some long range order in the direction of the molecular long axes while the molecules centers of gravity do not have a long range order. This direction is characterized with the so-called director, i.e. a unit vector function $\mathbf{n}(x, y, z, t)$ of coordinates (x, y, z) and time t in general case. The structure of NLC is presented in Fig. 1. Cholesteric liquid crystals (CLC) consist of chiral molecules. For this reason, they form a helical structure in such a way that the direction of the preferred molecular orientation rotates in space along the helical axis with a period of the order of magnitude of 300nm [2].

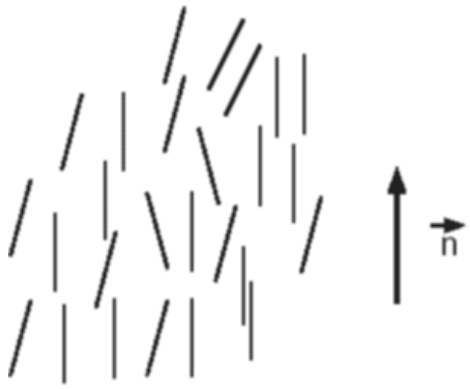

Figure 1: The molecular arrangement in NLC. $\mathbf{n}$ is the vector director defining the preferential direction of the molecular long axes.

The centers of gravity of CLC molecules centers also do not have a long range order, and CLC may be characterized as a form of twisted NLC. The structure of CLC is shown in Fig. 2.

The optics of CLC as a helical structure is of a special interest. It has been thoroughly investigated theoretically [1, 2, 4, 5].

Unlike NLC and CLC having only orientational long-range order, smectic liquid crystals possess a layered structure. The layer thickness is approximately equal to a length of molecule along its long axis $d \sim (2 \div 3)\,\mathrm{nm}$. In smectic A liquid crystals (SA) the molecules are bound to the layers and their long axes are perpendicular to a layer plane. Inside a layer the molecules form a two-dimensional liquid. The SA structure is presented in Fig. 3.

We do not consider smectic C liquid crystals with tilted molecules in

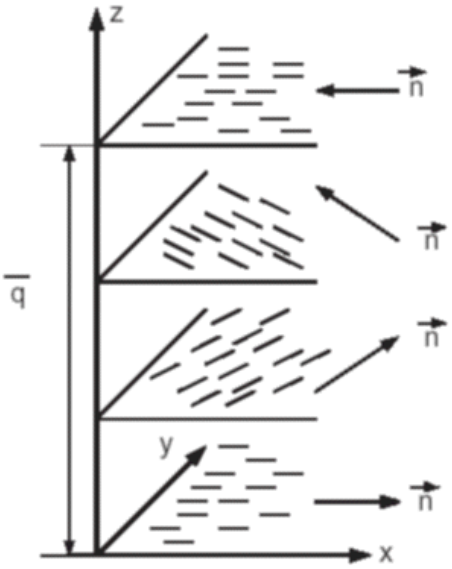

Figure 2: The arrangement of molecules in CLC. Here q is the pitch of the helix, or the inverse period.

layers, smectic B liquid crystals with in-layer hexagonal ordering of molecules, chiral smectic C liquid crystals with a spontaneous polarization and different exotic mesophases [1, 2]. LC sample orientation with respect to the boundary is called homeotropic when the molecular long axis is perpendicular to the boundary, or planar when the long molecular axis is parallel to it [1, 2]. The one-dimensional mass density wave in SA results in a complex order parameter where the modulus describes the mass density and the phase corresponds to the layer displacement. The layers can move relatively easy one along another since the elastic constant $B \sim \left(2 \times 10^7 \div 10^8\right) \mathrm{ergcm}^{-3}$ related to the layer compression is two, or three orders of magnitude less than the one responsible for the bulk compression [1, 2]. The elastic energy related to the director reorientation and the layer compression is determined by the layer displacement $u\left(x, y, z, t\right)$ along the direction perpendicular to a smectic layer plane. Due to the layer motion, there exist two practically uncoupled two acoustic modes in SA: an ordinary longitudinal sound caused by a bulk compression, and the so-called second sound (SS) caused by layer compression without the mass density change, which actually represents the oscillations of the complex order parameter phase [1]. The existence of

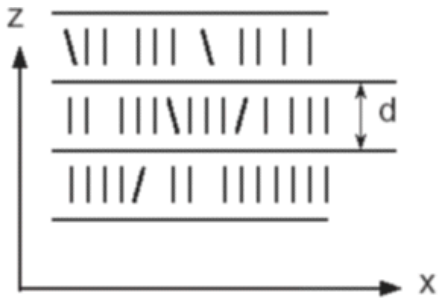

Figure 3: The arrangement of molecules in smectic A liquid crystal. Here d is a layer thickness.

SS was theoretically predicted by de Gennes [6], and then it was observed experimentally by means of spontaneous Brillouin scattering [7], acoustic measurements [8, 9], and Raleigh scattering [10, 11]. It has been shown that SS can be excited in a conducting SA [12, 3]. The SS mode is neither purely longitudinal, nor transverse, and it vanishes for the wave vectors parallel or perpendicular to the layer plane [1, 2].

LC are highly nonlinear materials due to their unique complex physical structures. Their physical properties such as temperature, molecular orientation, mass density are easily perturbed by an applied optical field. The nonlinear optics of LC emerged as a separate field of liquid crystals study in the early seventies of the 20-th century. As early as in 1973-1974 the light self-focusing in an isotropic phase of NLC was registered [13 - 15]. LC have been singled out as promising materials for nonlinear optics due to their large optical nonlinearity even in an isotropic phase [16]. The first attempts to develop a theory of nonlinear optical effects in NLC were made in 1979 [17 - 19]. Since then, the nonlinear optical phenomena in LC have been thoroughly investigated both theoretically and experimentally, and an enormous number of books and papers have been published concerning mainly NLC. We do not intend to even briefly review this immense field. The history of the problem and the basic up-today results can be found in a series of excellent reviews and monographs [20 - 25]. NLC for a long time remained the main focus of nonlinear optical investigations and applications due to their giant orientational and thermal nonlinearity and their sensitivity to low light intensity [22, 24, 26]. They may be used in the image processing, as a core material in optical fibers, optical waveguides (see, for example, the works of I.C. Khoo and co-workers [27 - 35]. However, NLC have a slow

decay time of reorientation and large light scattering loss [24], which limits its possible applications of liquid crystals in high peak-power lasers, where elements are required to be low in loss, and to possess a fast response [36].

In SA, on the contrary, the electrostrictive mechanisms of the optical nonlinearity are predominant in the case of irradiation with high intensity nano- and picosecond laser pulses [37 - 39]. The Brillouin scattering in SA samples with a thickness of about $(25 \div 250)\,\mu$m characterized by a pumping intensity of about $100\mathrm{MWcm}^{-2}$ and pulse duration of about 20ns is accompanied by a strong acoustic excitation with an acoustic lifetime of about 100ns and a high gain due to the large electrostrictive constants of LC [37, 38]. For this reason, SA appear to be good candidates for small, fast and sensitive spatial light modulators operating at high enough light intensities.

The objective of this paper is to give a detailed review of theoretical results in the field of nonlinear optics of SA obtained during a rather long period of time, mainly by the author with co-workers. The choice of the topic is determined by two factors: (i) the personal interests of the author; (ii) the intention to attract the researchers attention to the possible applications of SA in optics. In a number of works [40 - 47] the nonlinear optical effects in SA caused by a specific mechanism of the cubic nonlinearity determined by the smectic layer normal displacement and propagating mode of SS were investigated theoretically. Self-focusing, self-trapping, stimulated light scattering (SLS), four wave mixing (FWM) [48], and related electrodynamic and hydrodynamic effects in SA have been considered. The mechanism mentioned above combines the typical characteristics of the orientational and electrostrictive nonlinearities, since it occurs without a change of a mass density, strongly depends on the light polarization and propagation direction, and, on the other hand, has a frequency dependence of a resonance form, short response time and the characteristic energy which is intermediate between the orientational energy and the bulk compression one. The advantages of this optical nonlinearity mechanism are following.

1. Large magnitude of the cubic nonlinearity in comparison with an ordinary Brillouin nonlinearity due to the smaller magnitude of the corresponding elastic constant.

2. Short time response similar to acoustic processes in isotropic liquids. The SS velocity $s_0 \sim 10^4\mathrm{cm/s}$, and the relaxation time $\tau \sim 10^{-6}\mathrm{s}$ for a wave number $k \sim 10^3\mathrm{cm}^{-1}$ [1, 2, 10, 11].

3. Weak temperature dependence, at least for temperatures not very close

to the phase transition.

4. Resonant form of the frequency dependence.

5. Strong dependence on the polarization and propagation direction of light beams due to the anisotropic dispersion relation of SS.

The results obtained are briefly enumerated below.

1. The nonlinear part of the SA refraction index responsible for the light beam self-focusing and self-trapping is one or two orders of magnitude greater than the one for the orientational Kerr effect and electrostriction in isotropic organic liquids.

2. The stimulated scattering of two incident arbitrary polarized light waves transforms into a partially degenerate FWM due to the splitting of each incident wave into the ordinary and extraordinary ones in a strongly anisotropic SA. The light waves coupled through the SS undergo the parametric energy exchange and cross-phase modulation. The gain coefficient of the signal waves is two orders of magnitude greater than the one in isotropic organic liquids. Estimations show that for the typical values of material parameters, the gain coefficient per unit intensity of the incident beam is $\sim (0.01 \div 10)$ cm/MW which yields for the intensity 100 MW/cm^2 the value of the gain coefficient $\sim \left(1 \div 10^3\right)$ cm^{-1} [44].

3. The nondegenerate FWM in SA due to the stimulated scattering on the SS is also possible. It is characterized by an especially complicated scattering spectrum due to the combination of anisotropy and nonlinearity. In the particular case of the counterpropagating waves and frequency balance a phase conjugation process occurs accompanied by the amplification of a phase-conjugate wave.

4. The light wave interference results in the creation of the dynamic grating of the layer displacement and excites a hydrodynamic flow.

5. The light - induced dynamic grating of the layer displacement, in turn, generates a longitudinal high-frequency electric field due to the so-called flexoelectric effect [1]. This electric field breaks the inversion symmetry of SA and permits the second harmonic generation.

6. In a weakly conducting SA the light-induced hydrodynamic flow crucially affects the electroconvection process. The electric current in SA

is mainly due to ions with a very low mobility $\mu \sim 10^{-10}$ $\mathrm{m}^2/\mathrm{V\,sec}$ [49]. The high frequency velocity of the light-induced hydrodynamic flow can be greater than the drift velocity of ions in a dc electric field with the magnitude of the order of $\left(10^3 \div 10^4\right)$ V/cm. As a result, the ac component of the electric current would be predominant, which makes the formation of high frequency patterns possible.

To our knowledge, until now the number of experimental works on SA nonlinear optics has been rather limited [38, 39, 50]. The theoretical results concerning the nonlinear optical effects in SA are in a good accord with the existing experimental results [38, 39, 50].

The paper is constructed as follows. In Section 2, the basic equations are introduced including the SA equation of motion and the nonlinear wave equation for the light wave. In Section 3, the light self-action effects in SA are discussed. In Section 4, the results concerning the nonlinear wave mixing are presented. In Section 5, the light induced electrohydrodynamic phenomena in SA are analyzed. The conclusions are presented in Section 6.

2 Basic equations

The theoretical description of non-linear optical effects in liquid crystals is based on the simultaneous solution of the Maxwell equations containing the non-linear polarization due to the mechanisms specific for liquid crystals and the equation of motion of the liquid crystal medium itself in the presence of the optical radiation [24, 48]. We are interested in the non-linear phenomena related to SS as it was mentioned above. We start with the hydrodynamics of SA thoroughly formulated in a number of works [1, 2, 50 - 54]. The X, Y axes are chosen to be in the layer plane, and the Z axis coincides with the optical axis perpendicular to the layer. Assuming SA to be an incompressible anisotropic liquid far from the phase transition point and under the constant temperature, the system of equations describing the SA hydrodynamics has the form [1, 2]

$$\frac{\partial v_i}{\partial x_i} = 0 \tag{1}$$

$$\rho \frac{\partial v_i}{\partial t} = -\frac{\partial \Pi}{\partial x_i} + \Lambda_i + \frac{\partial \sigma'_{ik}}{\partial x_i} \tag{2}$$

$$\Lambda_x = \Lambda_y = 0, \Lambda_z = -\frac{\delta F}{\delta u} \tag{3}$$

$$\sigma'_{ik} = \alpha_0 A_{ll}\delta_{ik} + \alpha_1 A_{zz}\delta_{iz} + \alpha_4 A_{ik} + \alpha_{56}\left(A_{zk}\delta_{iz} + A_{zi}\delta_{kz}\right) + \alpha_7 A_{ll}\delta_{iz}\delta_{kz} \tag{4}$$

$$A_{ik} = \frac{1}{2}\left(\frac{\partial v_i}{\partial x_k} + \frac{\partial v_k}{\partial x_i}\right) \tag{5}$$

$$v_z = \frac{\partial u}{\partial t} \tag{6}$$

where v_i,ρ, Π, Λ_i, σ'_{ik}, α_i, F are the hydrodynamic velocity, the mass density, the pressure, the generalized force density, the viscous stress tensor, the viscosity Leslie coefficients, and the free energy density, respectively. In the presence of an external electric field $\mathbf{E}$ the free energy density F has the form [2, 55]

$$F = \frac{1}{2}B\left(\frac{\partial u}{\partial z}\right)^2 + \frac{1}{2}K\left(\frac{\partial^2 u}{\partial x^2} + \frac{\partial^2 u}{\partial y^2}\right) - \frac{1}{8\pi}\varepsilon_{ik}E_iE_k \tag{7}$$

where K is the elastic constant related to molecular orientation, and ε_{ik} is the dielectric constant tensor linear on the layer deformations [1, 2, 6, 52]

$$\varepsilon_{xx} = \varepsilon_{yy} = \varepsilon_\perp + a_\perp\frac{\partial u}{\partial z}, \varepsilon_{zz} = \varepsilon_\parallel + a_\parallel\frac{\partial u}{\partial z} \tag{8}$$

$$\varepsilon_{xz} = \varepsilon_{zx} = -\varepsilon_a\frac{\partial u}{\partial x}, \varepsilon_{yz} = \varepsilon_{zy} = -\varepsilon_a\frac{\partial u}{\partial y}, \varepsilon_a = \varepsilon_\parallel - \varepsilon_\perp \tag{9}$$

where $\varepsilon_\parallel, \varepsilon_\perp$ are the diagonal components of a uniaxial SA dielectric tensor ε_{ik} along the optical axis and normal to it, respectively, and $a_\perp, a_\parallel$ are the phenomenological dimensionless coefficients of an order of magnitude of unity [6]. In our case the bulk compression is ignored $\Pi = 0$. For the typical values of the layer compression elastic constant $B \sim 10^8 \mathrm{erg/cm}^3$ and the Frank elastic constant $K \sim 10^{-6}$dyn [1, 2], $Kk^2 \ll B$ for any reasonable value of the orientational excitation wave number k. We are interested in the case when $\partial u/\partial z \neq 0$ and the contribution of the purely orientational mode energy into (7) can be neglected. The layer continuity condition (6) is specific to SS propagation in SA when the slow permeation process can be ignored [1, 2]. Taking into account these assumptions and combining equations (1)-(9), we obtain the equation of motion for the layer normal displacement $u\,(\mathbf{r},t)$ [40]. The detailed derivation of this equation is presented in Appendix A. The equation of motion has the form

$$-\rho\nabla^2\frac{\partial^2 u}{\partial t^2} + \left[\alpha_1\nabla_\perp^2\frac{\partial^2}{\partial z^2} + \frac{1}{2}\left(\alpha_4 + \alpha_{56}\right)\nabla^2\nabla^2\right]\frac{\partial u}{\partial t} + B\nabla_\perp^2\frac{\partial^2 u}{\partial z^2} =$$

$$= \frac{1}{8\pi}\nabla_\perp^2\left\{\frac{\partial}{\partial z}\left[a_\perp\left(E_x^2 + E_y^2\right) + a_\parallel E_z^2\right] - 2\varepsilon_a\left[\frac{\partial}{\partial x}\left(E_xE_z\right) + \frac{\partial}{\partial y}\left(E_yE_z\right)\right]\right\} \tag{10}$$

where $\nabla_\perp^2 = \left(\partial^2/\partial x^2\right) + \left(\partial^2/\partial y^2\right)$. The left-hand side (LHS) of equation (10) is the SS equation including the viscous damping terms. Its solution is the SS wave with the dispersion relation [1]

$$\Omega = s_0 k_s \sin\varphi \cos\varphi \tag{11}$$

where $\Omega, s_0 = \sqrt{B/\rho}, \mathbf{k}_s, \varphi$ are the SS frequency, velocity, wave vector, and the angle between $\mathbf{k}_s$ and the layer plane, respectively. It is seen that SS wave vanishes both in the case of propagation direction parallel to the layers and in the case of propagation direction perpendicular to them [1, 2]. The right-hand side (RHS) of (10) shows that the SS excitation with light waves is possible only in the case of their oblique incidence. The attenuation time τ of the SS wave in the high frequency limit $\Omega\tau \gg 1$ is

$$\tau = 2\rho \left[\alpha_1 \frac{\left(k_{sx}^2 + k_{sy}^2\right) k_{sz}^2}{k_s^2} + \frac{1}{2}\left(\alpha_4 + \alpha_{56}\right) k_s^2 \right]^{-1}. \tag{12}$$

For the typical values of the viscosity Leslie coefficients $\alpha_i \sim 1$Poise and mass density $\rho \sim 1\mathrm{gcm}^{-3}$ [1, 2, 52], this condition holds for k_s up to $10^3\mathrm{cm}^{-1}$. In the particular case when $\partial u/\partial z = 0$, the large elastic energy term related to the layer compression vanishes and we should take into account the small orientational energy, which is similar to the NLC case. Then the equation of motion reduces to the following one [42]

$$\rho\frac{\partial^2 u}{\partial t^2} - \frac{1}{2}\left(\alpha_4 + \alpha_{56}\right)\nabla_\perp^2 \frac{\partial u}{\partial t} + K\nabla_\perp^2 u =$$

$$= \frac{\varepsilon_a}{4\pi}\left[\frac{\partial}{\partial x}\left(E_x E_z\right) + \frac{\partial}{\partial y}\left(E_y E_z\right)\right] \tag{13}$$

The propagation and interaction of light waves in a non-linear medium is described by the Maxwell equations with the non-linear electric induction $\mathbf{D}^{NL}$. These equations yield the wave equation

$$\mathrm{curlcurl}\mathbf{E} + \frac{1}{c^2}\frac{\partial^2 \mathbf{D}^L}{\partial t^2} = -\frac{1}{c^2}\frac{\partial^2 \mathbf{D}^{NL}}{\partial t^2} \tag{14}$$

where c is the speed of light in vacuum, $\mathbf{D}^L = \left(\varepsilon_\perp E_x, \varepsilon_\perp E_y, \varepsilon_\parallel E_z\right)$, and

$$D_x^{NL} = a_\perp \frac{\partial u}{\partial z}E_x - \varepsilon_a \frac{\partial u}{\partial x}E_z,\ D_y^{NL} = a_\perp \frac{\partial u}{\partial z}E_y,\ D_z^{NL} = a_\parallel \frac{\partial u}{\partial z}E_z - \varepsilon_a \frac{\partial u}{\partial x}E_x. \tag{15}$$

For the analysis of the light wave $\mathbf{E} = \mathbf{e}\left[A\left(z\right)\exp i\left(\mathbf{kr}-\omega t\right)+c.c.\right]$, we use the slowly varying amplitude approximation (SVA) [48]:

$$\left|\frac{\partial^2 A}{dz^2}\right| \ll \left|k\frac{\partial A}{\partial z}\right|. \tag{16}$$

Here $\mathbf{e}$,$\mathbf{k}$,ω, $A = |A|\exp i\gamma$ are the polarization unit vector, wave vector, frequency, complex slowly varying amplitude of the light wave, respectively, and *c.c.* stands for complex conjugate. In the case of a light beam with $A\left(\mathbf{r}\right)$, the condition (16) is used together with the quasi-optical approximation [48]

$$\left|k\frac{\partial A}{\partial z}\right| \sim \left|\nabla_{\perp}^2 A\right|. \tag{17}$$

The slowly varying amplitudes of an infinite plane wave and a light beam propagated in a non-linear medium are described respectively with the following reduced equations [48]

$$-2ik_z\frac{\partial A}{\partial z}\left[1-e_z\frac{(\mathbf{ke})}{k_z}\right] = \left(\frac{\omega}{c}\right)^2\left(\mathbf{kD}^{NL}\right)\exp\left(-i\mathbf{kr}\right) \tag{18}$$

$$-2ik_z\frac{\partial A}{\partial z} - \nabla_{\perp}^2 A = \left(\frac{\omega}{c}\right)^2\left(\mathbf{kD}^{NL}\right)\exp\left(-i\mathbf{kr}\right). \tag{19}$$

3 Light self-action effects

The passage of a laser beam through a nonlinear optical material results in the intensity-dependent phase shift due to the intensity dependence of the refractive index [48]. This phenomenon causes the so-called self-action effects [56], namely:

1. self-focusing, or a change of the amplitude form;

2. self-trapping, or the transforming of a light beam into a stable filament with a constant width;

3. self-phase modulation, or a phase change;

4. change of the state of a beam polarization.

3.1 Self-focusing and self-trapping

We start with the case of the stationary self-focusing assuming the beam amplitude to be time-independent [48]. Such an approach is valid when the pulse duration τ_p is much larger than the typical nonlinearity relaxation time [56]. In our case this relaxation time τ (12) can be used with a characteristic perturbation dimension w instead of k_s^{-1}. We choose the SA optical axis to be the Z axis and the SA layer plane to be the XY plane. The XZ plane can be chosen to be the light beam incidence plane due to the D_∞ symmetry of SA [1]. In a uniaxial medium two types of a light wave with different dispersion relations can propagate [55]: an ordinary wave with the dispersion relation

$$k^2 = \frac{\omega^2}{c^2}\varepsilon_\perp \tag{20}$$

and an extra-ordinary wave with the dispersion relation

$$k_\perp^2\varepsilon_\perp + k_z^2\varepsilon_\parallel = \frac{\omega^2}{c^2}\varepsilon_\perp\varepsilon_\parallel. \tag{21}$$

In a uniaxial medium an extra-ordinary wave is polarized in the incidence plane, while the transverse component E_o perpendicular to the incidence plane containing the optical axis behaves as an ordinary wave. The light wave splitting into two waves is shown in Fig. 4.

For a slab-shaped [57] light beam they have the form

$$E_y = A_o\left(\mathbf{r}\right)\exp i\left(\mathbf{k}_o\mathbf{r}{-}\omega t\right) + c.c. \tag{22}$$

$$E_e = \mathbf{e}_e\left[A_e\left(\mathbf{r}\right)\exp i\left(\mathbf{k}_e\mathbf{r}{-}\omega t\right) + c.c.\right] \tag{23}$$

where $\mathbf{e}_e, \mathbf{k}_o, \mathbf{k}_e$ are the extra-ordinary wave polarization vector, the ordinary and extra-ordinary wave vectors, respectively. Equation of motion (10) in the chosen geometry and in the steady-state case reduces to

$$B\frac{\partial^2 u}{\partial z^2} = \frac{1}{4\pi}\left\{\left[\left(a_\parallel e_{ez}^2 + a_\perp e_{ex}^2\right)\frac{\partial}{\partial z} - 2\varepsilon_a e_{ex}e_{ez}\frac{\partial}{\partial x}\right]|A_e|^2 + a_\perp\frac{\partial\left|A_o\right|^2}{\partial z}\right\}. \tag{24}$$

The simultaneous solution of equations (19) and (24) for the slowly varying amplitudes $A_{o,e}$ is hardy possible, in particular, since the ordinary and extra-ordinary beams propagate in different directions. The ordinary beam propagation direction coincides with its wave vector $\mathbf{k}_o$ and may be described with the coordinates

$$x' = \left(\mathbf{k}_o\mathbf{r}\right)/k_0 = x\sin\theta_o + z\cos\theta_o; z' = -x\cos\theta_o + z\sin\theta_o \tag{25}$$

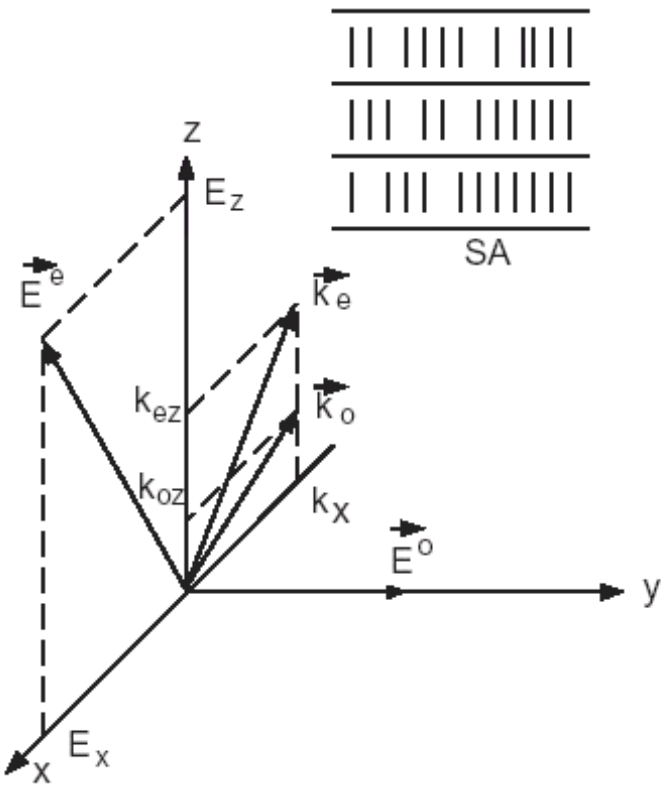

Figure 4: An arbitrary light wave is propagating in a uniaxial SA. Here $\mathbf{E}^e, \mathbf{E}^o, \mathbf{k}^e, \mathbf{k}^o$ are the electric field and the wave vectors of the extraordinary and ordinary wave, respectively.

where θ_o is the angle between $\mathbf{k}_o$ and the Z axis. The extraordinary beam in anisotropic medium propagates along the beam vector [55], which is determined by the angle $\theta_e = \arctan\left(\left(\varepsilon_\perp/\varepsilon_\parallel\right)\tan\theta_1\right)$ where θ_1 is the angle between $\mathbf{k}_e$ and the Z axis. We define this direction with the coordinates

$$x'' = x\sin\theta_e + z\cos\theta_e; z'' = -x\cos\theta_e + z\sin\theta_e. \tag{26}$$

Considering separately the ordinary and extra-ordinary beams one can obtain stable spatially localized solutions of the non-linear Schredinger equation (NSE) [58]. The self-focusing is possible for both the ordinary and extra-ordinary beams since the coefficients at the NSE cubic term are positive definite. The nonlinear parts n_{o2} and n_{e2} of the refractive indices in

both cases have the form, respectively [46, 47]

$$n_{o2} = \frac{a_\perp^2}{8\pi B k_o}; n_{e2} = h_e^2 \left[8\pi B \sqrt{\varepsilon_\perp \varepsilon_\parallel} \left(1 + \frac{\varepsilon_a}{\varepsilon_\perp} e_{ez} \sin\theta_e \right) \sin^2\theta_e \right]^{-1} \quad (27)$$

where $h_e = \left[a_\perp \left(e_{ex} \right)^2 + a_\parallel \left(e_{ez} \right)^2 \right] \sin\theta_e + 2\varepsilon_a e_{ex} e_{ez}$. For the typical values of material parameters, $\varepsilon_\perp, \varepsilon_\parallel \sim 2$ [24], $a_\perp, a_\parallel \sim 1$ [6], the nonlinear part (27) of of the refractive index may reach $3 \times 10^{-9} esu$ which is up to three orders of magnitude larger than a similar quantity in isotropic organic liquids [56, 57]. The localized self-trapped solutions, or the so-called spatial solitons [59], for the ordinary and extra-ordinary beams have the form, respectively [46, 47],

$$A_o = |A|_{\max} \exp i \left[\frac{a_\perp^2 |A|_{\max}^2 \omega^2}{16\pi B c^2 k_o} x' \right] \left(\cosh \left[\frac{a_\perp |A|_{\max} \omega}{2\sqrt{2}\pi B c} z' \right] \right)^{-1} \quad (28)$$

$$A_e = |A_e|_{\max} \exp i \left[\frac{h_e^2 |A|_{\max}^2 \omega^2}{16\pi B l_{e\parallel} c^2 \left(1 + \left(\varepsilon_a / \varepsilon_\perp \right) e_{ez} \sin\theta_e \right) \sin^2\theta_e} x'' \right]$$

$$\times \left(\cosh \left[\frac{h_e |A|_{\max} \omega}{2c\sqrt{2\pi B \left(1 + \left(\varepsilon_a / \varepsilon_\perp \right) e_{ez} \sin\theta_e \right)} \sin\theta_e} z'' \right] \right)^{-1} \quad (29)$$

where $l_{e\parallel} = k_{e\parallel} \left(1 + \left(\varepsilon_a / \varepsilon_\perp \right) e_{ez} \sin\theta_e \right)^{-1}$. The widths w_o and w_e of these solitons are, respectively,

$$w_o = \frac{2\sqrt{2}\pi B c}{a_\perp |A|_{\max} \omega}; w_e = \frac{2c\sqrt{2\pi B \left(1 + \left(\varepsilon_a / \varepsilon_\perp \right) e_{ez} \sin\theta_e \right)} \sin\theta_e}{h_e |A|_{e\max} \omega}. \quad (30)$$

Numerical evaluations show that for the power $P_{cr} \sim 2 \times 10^2$Watt the width $w_o, w_e \sim 10^{-2}$cm. The SA samples of such a thickness are feasible [38, 11]. The ordinary light beam self-trapping in the form of a bright surface wave

$$A\left(z\right) = \left| A\left(z_0\right) \right| \left[\cosh \left(\frac{z - z_0}{w_o} \right) \right]^{-1} \quad (31)$$

at the boundary $z = 0$ of an isotropic homogeneous medium $z < 0$ and the SA cladding $z > 0$, is also possible when the medium dielectric constant $\varepsilon_s > \varepsilon_\perp$ [46, 47]. Here $z_0 > 0$ is the intensity maximum position inside the SA cladding.

3.2 Spatial self-phase modulation and polarization change

In the specific case when the layer normal deformation is absent: $du/dz = 0$, and the arbitrary polarized light wave is propagated in a layer plane XY the spatial phase modulation occurs due to the interaction of the optical field components that are parallel and perpendicular to the optical axis [47]. These components excite the static grating of layer tangential deformations similar to the director deviations in NLC. The optical field components coupled through this grating undergo spatial phase modulation. Due to the field-induced phase change, the phase difference between the ordinary and extra-ordinary beam is changing, which results in the polarization change of the light beam propagated in SA. Using the Stokes parameters [60] $S_{0,1,2,3}$ we get in our case [47]

$$S_{0,1} = |A_o|^2 \pm |A_e|^2 \,,\; S_2 = 2\,|A_o A_e| \cos\varrho,\; S_3 = 2\,|A_o A_e| \sin\varrho \tag{32}$$

where the phase difference ϱ is caused by anisotropy and nonlinearity [47]

$$\varrho = \Delta k_x x + \left(\frac{\omega}{c}\right)^2 \frac{\varepsilon_a^2 e_x^2}{8\pi K \left(\Delta k_x\right)^2 k_{ox} k_{ex}} \left(k_{ox}^2 \left|A_o\right|^2 - k_{ex}^2 \left|A_e\right|^2\right) x \tag{33}$$

where $\Delta k_x = k_{ox} - k_{ex}$. It is seen from (33) that the first term is caused by the SA anisotropy as in any optically uniaxial medium, except that it has in our case a larger magnitude due to the extremely large optical anisotropy of liquid crystals $\Delta\varepsilon \sim 0.2$ [24]. The second term is light-induced, and it emerges due to the spatial self-phase modulation related to layer tangential deformations. The polarization ellipse form and axes directions characterized with the orientation angle Ψ and ellipticity angle χ [60] depend on the distance in the following way

$$\tan 2\Psi = \frac{S_2}{S_1} = \frac{2\,|A_o A_e| \cos\varrho}{|A_o|^2 - |A_e|^2},\; \tan 2\chi = \frac{S_2}{S_0} = \frac{2\,|A_o A_e| \cos\varrho}{|A_o|^2 + |A_e|^2} \tag{34}$$

which clearly shows the nonlinear change of the light beam polarization. For a moderate intensity level the nonlinear terms can be singled out explicitly by the expansion in powers of $\cos\varrho$.

4 Non-linear wave-mixing in SA

4.1 General approach

We consider the non-linear optical wave-mixing in SA due to the specific mechanism of an optical non-linearity related to a light-induced layer normal displacement $u\left(\mathbf{r}, t\right)$ [40 - 47]. In the simplest case when both light waves

are polarized in either the incidence plane, or normal to it, a two-wave mixing occurs [40 - 45]. In the general case, an arbitrary polarized light wave propagating in a uniaxial medium splits into ordinary and extra-ordinary waves as it was mentioned above. As a result, the non-linear two-wave mixing transforms into a kind of FWM defined as a partially degenerate FWM since there are four waves with two essentially different frequencies [44]. In the case of four incident waves with frequencies differing by a quantity close to the SS frequency, a kind of Brillouin-enhanced FWM occurs [45]. In all these cases the interfering light waves create a dynamic grating of a layer normal displacement $u(\mathbf{r}, t)$ according to equation (10). In the case of the partially degenerate FWM such a grating consists of four harmonics with the same frequency and different wave vectors. This grating reduces to the one single harmonic in the case of an ordinary two-wave mixing. In the case of the Brillouin-enhanced FWM, there exist 6 harmonics with the essentially different frequencies and wave vectors. The fundamental light waves undergo the cross-phase modulation and parametric amplification (attenuation) due to the coupling through the light-induced dynamic grating $u(\mathbf{r}, t)$. A spectrum of Brillouin-like harmonics with the Stokes and anti-Stokes frequencies and combination wave vectors emerges.

The total electric field $\mathbf{E}^{tot}$ in SA can be presented as a finite number of harmonics with SVA including the fundamental waves $\mathbf{E}_m$, additional components $\mathbf{E}'_m$ of the fundamental waves caused by the combined effect of anisotropy and nonlinearity, and Brillouin-like scattered harmonics $\mathbf{f}_l^S$:

$$\mathbf{E}^{tot} = \sum_m \left(\mathbf{E}_m + \mathbf{E}'_m\right) + \sum_l \mathbf{f}_l^S. \tag{35}$$

The light absorption in SA can be neglected [24]. The fast relaxation of SS due to SA high viscosity makes it possible to consider the stimulated light scattering (SLS) on SS as a steady state process and ignore the time dependence of SVA. The non-linear part of the electric induction $\mathbf{D}^{NL}$ (15) represents a Fourier series containing a finite number of harmonics

$$\mathbf{D}^{NL} = \sum_l \left(\mathbf{D}_l^{NL} \exp i\psi_l + c.c.\right). \tag{36}$$

The non-linear interaction between the light waves is efficient only in the case of the phase matching which occurs when the energy and momentum conservation conditions are fulfilled for the frequencies and wave vectors of the coupled waves [48]. In the case of SLS on the light-induced dynamic grating these conditions are met automatically for the frequencies and wave

vectors of the fundamental waves. As a result, the non-linear induction $\mathbf{D}^{NL}$ (36) and the field $\mathbf{E}^{tot}$ contain both the phase matched terms and some other terms with the combination frequencies and wave vectors. The non-linear induction $\mathbf{D}^{NL}$ gives rise to three types of non-linear optical effects: (i) the parametric amplification and cross-phase modulation determined by the phase matched terms $\mathbf{D}^{NL}$ components parallel to the electric field of the fundamental waves; (ii) the additional component generation caused by the phase matched terms $\mathbf{D}^{NL}$ components perpendicular to the electric field of the fundamental waves; (iii) the Brillouin-like scattering due to the non-linear terms with the combination frequencies and wave vectors. Substituting (35) and (36) into wave equation (14), taking into account the SVA approximation (16), and equating the phase matched terms in the both sides of (14), we obtain three sets of equations describing the effects mentioned above [44, 45, 47]: the reduced equations for the SVA of the fundamental waves, the wave equations for the additional components $\mathbf{E}'_m$, and the wave equations for the scattered harmonics $\mathbf{f}_l^S$. In our case the cubic susceptibility represents a complex tensor [45], which does not permit an explicit solution. The system has only one integral of motion, and as a result, each phase evolves independently. The SS modes are passive, or "slaved", and the scale separation exists between the dissipation and excitation processes [61]. The energy exchange occurs on a SS wave excitation length $L_E \gg L_D = s_0\tau$ where L_D is the SS dissipation length, and it is non-reciprocal, unlike the situation in conservative systems [62].

4.2 Partially degenerate FWM

Consider two incident light waves $\mathbf{E}_{1,2}^I$ propagated from a free space $z < 0$ to SA filling a semi-space $z > 0$:

$$\mathbf{E}_{1,2}^I = \mathbf{e}_{1,2}^I \left[A_{1,2}^I \exp i\left(\mathbf{k}_{1,2}^I \mathbf{r} - \omega_{1,2} t\right) + c.c.\right] \tag{37}$$

where $k_{1,2}^I = \omega_{1,2}/c$. We define for the sake of definiteness $\omega_1 > \omega_2$, $\Delta\omega = \omega_1 - \omega_2 \ll \omega_1$, and the unit polarization vectors $\mathbf{e}_{1,2}^I$ are assumed to be three-dimensional. The plane of incidence for one of the waves (37) may be chosen to be the XZ plane which is possible due to the D_∞ symmetry of SA permitting any rotation around the optical Z axis [1]. The second wave in general case is propagated in an arbitrary plane and has a three-dimensional wave vector. In this geometry, each wave inside SA splits into two waves: an ordinary wave polarized perpendicular to the optical axis and an extraordinary one which possesses the component parallel to the optical axis, as

was mentioned above. As a result, four waves propagate in SA:

$$\mathbf{E}_1^{o,e} = \mathbf{e}_1^{o,e} \left[A_1^{o,e}(z) \exp i \left(\mathbf{k}_1^{o,e} \mathbf{r} - \omega_1 t \right) + c.c. \right] \tag{38}$$

$$\mathbf{E}_2^{o,e} = \mathbf{e}_2^{o,e} \left[A_2^{o,e}(z) \exp i \left(\mathbf{k}_2^{o,e} \mathbf{r} - \omega_2 t \right) + c.c. \right] \tag{39}$$

Here the slowly varying complex amplitudes have the form

$$A_{1,2}^{o,e}(z) = \left| A_{1,2}^{o,e}(z) \right| \exp i\gamma_{1,2}^{o,e} \tag{40}$$

The geometry of the problem is shown in Fig.5.

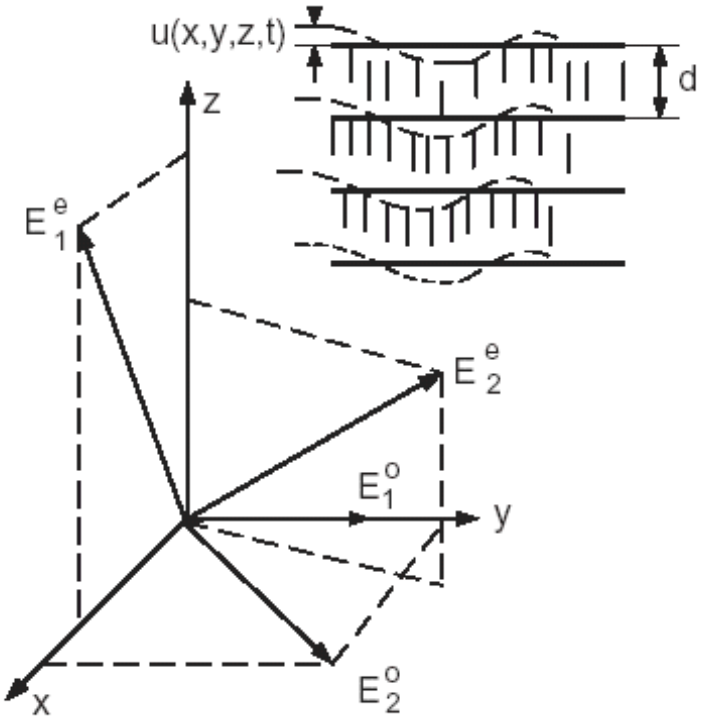

Figure 5: The geometry of SLS in SA. Here $\mathbf{E}_1^{e,o}, \mathbf{E}_2^{e,o}$ are extraordinary and ordinary components of each incident light wave, and $u(x, y, z, t)$ is a layer normal displacement.

The solution of reduced equations (18) for the waves (38), (39) with the non-linear polarization (15) yields the integral of motion [44]

$$W_1^o + W_1^e + W_2^o + W_2^e = 1 \tag{41}$$

where

$$W_{1,2}^{o,e} = \frac{c^2 l_{1,2}^{o,e}}{\omega_{1,2}^2 I_0} \left| A_{1,2}^{o,e} \right|^2 \tag{42}$$

$$I_0 = \frac{c^2}{\omega_1^2} \left(l_1^o \left| A_1^o \right|^2 + l_1^e \left| A_1^e \right|^2 \right) + \frac{c^2}{\omega_2^2} \left(l_2^o \left| A_2^o \right|^2 + l_2^e \left| A_2^e \right|^2 \right) = const \tag{43}$$

and $l_{1,2}^o = k_{1,2z}^o, l_{1,2}^e = k_{1,2z}^e \left[1 - e_{1,2z}^e \left(\mathbf{k}_{1,2}^e \mathbf{e}_{1,2}^e \right) / k_{1,2z}^e \right]$. The system of the coupled reduced equations of the type (18), along with the condition (41), yields [44]

$$W_1^{o,e}(z) = W_1^{o,e}(0) \exp \left[- \int_0^z \left(\beta_{3,2} W_2^{o,e} + \beta_{4,1} W_2^{e,o} \right) dz' \right] \tag{44}$$

$$W_2^{o,e}(z) = W_2^{o,e}(0) \exp \left[\int_0^z \left(\beta_{3,2} W_1^{o,e} + \beta_{1,4} W_1^{e,o} \right) dz' \right] \tag{45}$$

$$\gamma_1^{o,e}(z) - \gamma_1^{o,e}(0) = -\frac{1}{2} \int_0^z \left(\delta_{3,2} W_2^{o,e} + \delta_{4,1} W_2^{e,o} \right) dz' \tag{46}$$

$$\gamma_2^{o,e}(z) - \gamma_2^{o,e}(0) = -\frac{1}{2} \int_0^z \left(\delta_{3,2} W_1^{o,e} + \delta_{1,4} W_1^{e,o} \right) dz' \tag{47}$$

where the coupling constants are

$$\beta_j = \frac{\omega_1^2 \omega_2^2 I_0 \Delta\omega h_j^2 \left(\Delta k_{j\perp} \right)^2 \Gamma_j}{4\pi\rho \left(\Delta k_j \right)^2 \left| G_j \right|^2 c^4 d_j} > 0; \; \delta_j = \frac{\omega_1^2 \omega_2^2 I_0 \left[(\Delta\omega)^2 - \Omega_j^2 \right] h_j^2 \left(\Delta k_{j\perp} \right)^2}{4\pi\rho \left(\Delta k_j \right)^2 \left| G_j \right|^2 c^4 d_j} \tag{48}$$

$d_1 = l_1^e l_2^o, d_2 = l_1^e l_2^e, d_3 = l_1^o l_2^o, d_4 = l_1^o l_2^e,$

$$h_1 = a_\perp \Delta k_{1z} e_{1x}^e e_{2x}^o - \varepsilon_a \left(\Delta k_{1x} e_{1z}^e e_{2x}^o + \Delta k_{1y} e_{1z}^e e_{2y}^o \right) \tag{49}$$

$$\begin{aligned} h_2 = a_\perp \Delta k_{2z} e_{1x}^e e_{2x}^o + a_\parallel \Delta k_{2x} e_{1z}^e e_{2z}^e - \\ - \varepsilon_a \left[\Delta k_{2x} \left(e_{1x}^e e_{2z}^e + e_{1z}^e e_{2x}^e \right) + \Delta k_{2y} e_{1z}^e e_{2y}^e \right] \end{aligned} \tag{50}$$

$$h_3 = a_\perp \Delta k_{3z} e_{2y}^o; \; h_4 = a_\perp \Delta k_{4z} e_{2y}^e - \varepsilon_a \Delta k_{4y} e_{2z}^e \tag{51}$$

$$\Delta\mathbf{k}_1 = \mathbf{k}_1^e - \mathbf{k}_2^o; \; \Delta\mathbf{k}_2 = \mathbf{k}_1^e - \mathbf{k}_2^e; \; \Delta\mathbf{k}_3 = \mathbf{k}_1^o - \mathbf{k}_2^o; \; \Delta\mathbf{k}_4 = \mathbf{k}_1^o - \mathbf{k}_2^e. \tag{52}$$

The denominator of the Fourier transform of SS Green function G_j is given by

$$G_j = (\Delta\omega)^2 - \Omega_j^2 + i\Delta\omega\Gamma_j;\ j = 1,..,4 \tag{53}$$

where the SS frequency Ω_j and the temporal decay constant Γ_j have the form, respectively

$$\Omega_j^2 = s_0^2 \frac{(\Delta k_{j\perp})^2 (\Delta k_{jz})^2}{(\Delta k_j)^2} \tag{54}$$

$$\Gamma_j = \frac{1}{\rho}\left[\alpha_1 \frac{(\Delta k_{j\perp})^2 (\Delta k_{jz})^2}{(\Delta k_j)^2} + \frac{1}{2}(\alpha_4 + \alpha_{56})(\Delta k_j)^2\right]. \tag{55}$$

The dynamic grating wave vectors $\Delta\mathbf{k}_j$ are determined by relations (52) and $(\Delta k_{j\perp})^2 = (\Delta k_{jx})^2 + (\Delta k_{jy})^2$. The comparison of equations (41) and (44), (45) shows that

$$z \to \infty,\ W_1^{o,e} \to 0, W_2^o + W_2^e \to 1 \tag{56}$$

The limiting values (56) show that, due to the non-linear wave mixing, the parametric entire energy transfer occurs from the pumping pair of light waves with the higher frequency ω_1 to the signal pair of waves with the lower frequency ω_2. The coupled light waves form a macroscopically squeezed state. Relations (46) and (47) manifest a coupled light waves cross phase modulation. It is seen from equations (44), (45), (48) and (53) that the especially strong coupling between the pair of light waves occurs in the resonance case determined by the condition

$$(\Delta\omega)^2 = \Omega_j^2. \tag{57}$$

The phase of the pumping wave is rapidly increasing and tends to infinity while the signal wave phase tends to a finite constant value. The detailed analysis of the reduced eqautions is presented in Appendix B.

Consider the practically important case when each of the incident light waves (38), (39) is polarized predominantly in the incidence plane or perpendicular to it while the other components are small. For the sake of definiteness, we assume that the pumping wave $\mathbf{E}_1^I$ is mainly polarized in the incidence plane and the signal wave $\mathbf{E}_2^I$ is mainly polarized normal to its incidence plane [44]. In such a case we get

$$W_1^e \gg W_1^o,\ W_2^o \gg W_2^e. \tag{58}$$

The quantities W_1^e and W_2^o can be expanded into a series

$$W_1^e = W_{10}^e + W_{11}^e + ..., |W_{11}^e| \ll |W_{10}^e| \tag{59}$$

$$W_2^o = W_{20}^o + W_{21}^o + ..., |W_{21}^o| \ll |W_{20}^o| \tag{60}$$

because in the general case all intensities are finite and converge at large z as it is seen from (56). The chain of the coupled reduced equations yields in the first and the second approximations, respectively [44]

$$W_{10}^e = \frac{[W_1^e(0) + W_2^o(0)]}{2}[1 - \tanh(\eta - \eta_0)],$$

$$W_{20}^o = \frac{[W_1^e(0) + W_2^o(0)]}{2}[1 + \tanh(\eta - \eta_0)] \tag{61}$$

$$W_2^e = W_2^e(0)\left[\frac{\cosh(\eta_0)\exp(\eta)}{\cosh(\eta - \eta_0)}\right]^{b_1},\ W_1^o = W_1^o(0)\left[\frac{\cosh(\eta_0)\exp(-\eta)}{\cosh(\eta - \eta_0)}\right]^{b_2} \tag{62}$$

$$W_{11}^e = \frac{1}{[\cosh(\eta - \eta_0)]^2}\int_0^\eta d\eta' \left[\cosh\left(\eta' - \eta_0\right)\right]^2 \left[1 - \tanh\left(\eta' - \eta_0\right)\right]$$

$$\times [W_1^o + W_2^e(1 - b_1) - W_1^o(0) - W_2^e(0)] \tag{63}$$

$$W_{21}^o = \frac{1}{[\cosh(\eta - \eta_0)]^2}\int_0^\eta d\eta' \left[\cosh\left(\eta' - \eta_0\right)\right]^2 \left[1 + \tanh\left(\eta' - \eta_0\right)\right]$$

$$\times [W_1^o(0) + W_2^e(0) - W_2^e - W_1^o(1 - b_2)] \tag{64}$$

where $b_{1,2} = \beta_{2,3}/\beta_1, \eta = \beta_1 [W_1^e(0) + W_2^o(0)] z/2$ and the crossing point z_0 is determined by

$$z_0 = \frac{1}{\beta_1}\ln\left[\frac{W_1^e(0)}{W_2^o(0)}\right]. \tag{65}$$

The explicit evaluation of integrals (63) and (64) is hardly possible. However, the analysis shows that the quantities W_{11}^e, W_{21}^o are finite, small and satisfy the conservation law (41). The system is stable with respect to both the thickness of SA sample and the pumping intensity [44]. The phases $\gamma_1^{o,e}$ of the pumping waves $\mathbf{E}_1^{o,e}$ rapidly increase at $\eta \to \pm\infty$ which means that the pumping waves depletion is accompanied by their amplitudes oscillations. The phases $\gamma_2^{o,e}$ of the signal waves $\mathbf{E}_2^{o,e}$ tend to a constant value at large η, and the amplification saturates at almost constant phases.

The spectrum of the Brillouin-like scattered harmonics $\mathbf{f}_l^S = \mathbf{F}_l^S \exp i\psi_l +$ *c.c.* consists of 12 terms with the Stokes and anti-Stokes frequencies $\omega_S = 2\omega_2 - \omega_1$ and $\omega_A = 2\omega_1 - \omega_2$ and 8 terms with the fundamental frequencies

$\omega_{1,2}$ and combination wave vectors. These harmonics have the following phases ψ_l [44]:

$$\left[\left(2\mathbf{k}_2^e - \mathbf{k}_1^{o,e}\right)\mathbf{r} - \omega_S t\right]; \left[\left(2\mathbf{k}_2^o - \mathbf{k}_1^{o,e}\right)\mathbf{r} - \omega_S t\right]; \left[\left(\mathbf{k}_2^o + \mathbf{k}_2^e - \mathbf{k}_1^{o,e}\right)\mathbf{r} - \omega_S t\right] \quad (66)$$

$$\left[\left(2\mathbf{k}_1^e - \mathbf{k}_2^{o,e}\right)\mathbf{r} - \omega_A t\right]; \left[\left(2\mathbf{k}_1^o - \mathbf{k}_2^{o,e}\right)\mathbf{r} - \omega_A t\right]; \left[\left(\mathbf{k}_1^o + \mathbf{k}_1^e - \mathbf{k}_2^{o,e}\right)\mathbf{r} - \omega_A t\right] \quad (67)$$

$$\left[\left(\mathbf{k}_2^e - \mathbf{k}_2^o + \mathbf{k}_1^{o,e}\right)\mathbf{r} - \boldsymbol{\omega}_1 t\right]; \left[\left(\mathbf{k}_2^o - \mathbf{k}_2^e + \mathbf{k}_1^{o,e}\right)\mathbf{r} - \boldsymbol{\omega}_1 t\right] \quad (68)$$

$$\left[\left(\mathbf{k}_1^e - \mathbf{k}_1^o + \mathbf{k}_2^{o,e}\right)\mathbf{r} - \boldsymbol{\omega}_2 t\right]; \left[\left(\mathbf{k}_1^o - \mathbf{k}_1^e + \mathbf{k}_2^{o,e}\right)\mathbf{r} - \boldsymbol{\omega}_2 t\right]. \quad (69)$$

The additional components $\mathbf{f}_1^o$, f_{1y}^e and f_{2z}^o emerging due to both the anisotropy and nonlinearity, are driven by the non-linear part of the electric induction $\mathbf{D}^{NL}$. The explicit expressions of the scattered harmonics and additional components are too involved [44], and we do not present them here. All these harmonics are spatially localized and vanish as $z \to \infty$.

In the particular case when two coupled waves are strictly polarized either in the incidence plane, or normal to it, the reduced equations can be solved explicitly, and the solution in a closed form has been obtained [40]-[43]. For the sake of definiteness, consider the two wave mixing of the extraordinary wave $\mathbf{E}_1^e$ polarized in the incidence plane and ordinary wave $\mathbf{E}_2^o$ polarized perpendicular to it. Then the conservation law (41) reduces to

$$W_1^e(0) + W_2^o(0) = 1 \quad (70)$$

and the solution takes the form

$$W_1^e = \frac{1}{2}\left[1 - \tanh\left(\eta - \eta_0\right)\right], W_2^o = \frac{1}{2}\left[1 + \tanh\left(\eta - \eta_0\right)\right] \quad (71)$$

$$\gamma_1^e - \gamma_1^e(0) = \frac{\delta_1}{2\beta_1} \ln\left[\frac{\cosh\left(\eta_0\right)\exp\left(-\eta\right)}{\cosh\left(\eta - \eta_0\right)}\right] \quad (72)$$

$$\gamma_2^o - \gamma_2^o(0) = \frac{\delta_1}{2\beta_1} \ln\left[\cosh\left(\eta_0\right)\exp\left(-\eta\right)\cosh\left(\eta - \eta_0\right)\right]. \quad (73)$$

The optical transmission losses in SA are caused mainly by two mechanisms: light absorption and light scattering on the orientational fluctuations [24]. The off-resonance light absorption in SA is comparatively small $\sim \left(10^{-2} \div 10^{-1}\right)$ cm^{-1}, while the orientational scattering in SA is considerably less than in NLC due to the higher degree of a molecular ordering [24]. Hence, the losses can be neglected when the coupling of strong incident waves is considered. However, it is instrumental to evaluate the threshold of the Brillouin like stimulated light scattering accompanied by the excitation

of a scattered Stokes wave $\mathbf{E}_2^e$ and SS wave by the strong pumping wave $\mathbf{E}_1^e$ (23)

$$u\left(\mathbf{r},t\right)=U\left(z\right)\exp i\left(\mathbf{k}_s\mathbf{r}-\Omega t\right)+c.c. \tag{74}$$

Analysis [41] shows that the excitation of $\mathbf{E}_2^e$ and $u\left(\mathbf{r},t\right)$ occurs when

$$\frac{\left|A_1^e\right|^2}{B}>\frac{4\pi k_{sz}^2\Gamma_2\left[\varepsilon_\perp'\left(e_{2x}^e\right)^2+\varepsilon_\parallel'\left(e_{2z}^e\right)^2\right]}{h_{2e}^2\Omega} \tag{75}$$

where $\varepsilon_\perp', \varepsilon_\parallel'$ are the imaginary parts of the permittivity describing the light absorption. Inequality (75) is similar to the condition of the stimulated Brillouin scattering on an ordinary sound [63, 64]. For SA, the losses caused by orientational scattering can be neglected [24]. The numerical estimations show that the threshold intensity value $c\left|A_{1thr}^e\right|^2/4\pi\sim 1\mathrm{MWcm}^{-2}$ which is less than the intensity threshold for an ordinary sound excitation in organic liquids such as n-hexane, carbon disulfide, etc. [63]. The amplitude gain coefficient g_2 has the form [41]

$$g_2=\frac{\left|A_1^e\right|^2\omega_2^2\Omega h_{2e}^2}{8\pi l_2^e c^2 k_{sz}^2\Gamma_2}. \tag{76}$$

In the particular case when both light waves

$$\mathbf{E}_1=\mathbf{e}_1\left[A_1\left(x\right)\exp i\left(k_{1x}x+k_{1y}y-\omega_1 t\right)+c.c.\right] \tag{77}$$

$$E_2=E_z=A_2\left(x\right)\exp i\left(k_{1x}x+k_{1y}y-\omega_2 t\right)+c.c. \tag{78}$$

are propagated in a layer plane of a planary oriented [1] SA sample, a stimulated scattering occurs on a so-called undulation mode [42]. In such a case SS wave vanishes since $k_{sz}=0$, $\partial u/\partial z=0$ and the overdamped undulation mode exists

$$u=U\left(x\right)\exp i\left(\Delta\mathbf{k}\mathbf{r}-\Delta\omega t\right)+c.c. \tag{79}$$

determined by equation (13). The SLS is similar to the one on the director oscillations in NLC and does not have a resonant character. The expressions for the amplitudes $A_{1,2}\left(x\right)$ have been obtained [42]. The amplification of the signal wave (78) is the strongest when

$$\Delta\omega=\omega_1-\omega_2\ll\Gamma_2\sim\Omega_2. \tag{80}$$

4.3 Four wave mixing in SA

Consider now a nondegenerate FWM in SA when four fundamental light waves

$$\mathbf{E}_m = \mathbf{e}_m \left[A_m \exp i \left(\mathbf{k}_m \mathbf{r} - \boldsymbol{\omega}_m t \right) + c.c. \right], \; m = 1, .., 4 \tag{81}$$

have close frequencies with the difference

$$\Delta\omega_{mn} = \omega_m - \omega_n \sim \frac{s_0}{c}\omega_m \ll \omega_m. \tag{82}$$

The geometry of the problem is similar to the one shown in Fig. 5 except that all light waves now have different frequencies. Suppose for the sake of definiteness that $\omega_1 < \omega_2 < \omega_3 < \omega_4$. Such a case is essentially different from the partially degenerate FWM [45]. The light wave with the lowest frequency ω_1 is amplified up to a saturation level, the light wave with the largest frequency ω_4 is depleted while the waves with the intermediate frequencies $\omega_{2,3}$ are compressed in space forming the soliton-like envelopes [45]. One may say that the four coupled waves form a kind of macroscopic squeezed states. Evidently, each arbitrary polarized wave in SA splits into an ordinary and extra-ordinary wave as was mentioned above, and FWM transforms into eight wave coupling. We do not discuss such a case and assume that all fundamental waves (81) are either polarized perpendicular to the incidence plane XZ and propagate as ordinary waves, or belong to the incidence plane XZ and behave as extra-ordinary waves. In the first case the polarization vectors $\mathbf{e}_m$ and the dispersion relations are, respectively

$$\mathbf{e}_m = \mathbf{e}_m^o = (e_{mx}, e_{my}, 0) \, ; \; (k_m^o)^2 = \frac{\omega_m^2}{c^2}\varepsilon_\perp. \tag{83}$$

In the second case we get

$$\mathbf{e}_m = \mathbf{e}_m^e = (e_{m\perp}^e, e_{mz}^e) \, ; \; \frac{(k_{m\perp}^e)^2}{\varepsilon_\parallel} + \frac{(k_{mz}^e)^2}{\varepsilon_\perp} = \frac{\omega_m^2}{c^2}; \; \mathbf{k}_{m\perp}^e = (k_{mx}, k_{my}) \tag{84}$$

Both cases differ by the form of the coupling constants h_{mn}. We consider first the extra-ordinary wave mixing. The dynamic grating of a layer displacement consisting of 6 harmonics has the form [45]

$$u\left(\mathbf{r},t\right) = \sum_{m,n,m\neq n} U_{mn} \exp i \left(\Delta\mathbf{k}_{mn}\mathbf{r} - \Delta\omega_{mn} t \right) \tag{85}$$

where $\Delta\mathbf{k}_{mn} = \mathbf{k}_m - \mathbf{k}_n$,

$$U_{mn} = \frac{i h_{mn}^e \left(\Delta k_{mn\perp} \right)^2}{4\pi\rho G_{mn} \left(\Delta k_{mn} \right)^2} A_m A_n^* \tag{86}$$

$$h_{mn} = \left[a_{\perp}\left(\mathbf{e}^{e}_{m\perp}\mathbf{e}^{e}_{n\perp}\right) + a_{\parallel}\left(e^{e}_{mz}e^{e}_{nz}\right)\right]\Delta k_{mnz} - \\ -\varepsilon_a\left[e^{e}_{mz}\left(\Delta\mathbf{k}_{mn}\mathbf{e}^{e}_{n\perp}\right) + e^{e}_{nz}\left(\Delta\mathbf{k}_{mn\perp}\mathbf{e}^{e}_{n\perp}\right)\right] \quad (87)$$

$$G_{mn} = \left(\Delta\omega_{mn}\right)^2 - \Omega^2_{mn} + i\Delta\omega_{mn}\Gamma_{mn};\ \Omega^2_{mn} = s_0^2\frac{\left(\Delta k_{mnz}\Delta k_{mn\perp}\right)^2}{\left(\Delta k_{mn}\right)^2} \quad (88)$$

$$\Gamma_{mn} = \frac{1}{\rho}\left[\alpha_1\frac{\left(\Delta k_{mnz}\Delta k_{mn\perp}\right)^2}{\left(\Delta k_{mn}\right)^2} + \frac{\left(\alpha_4+\alpha_{56}\right)}{2}\left(\Delta k_{mn}\right)^2\right]. \quad (89)$$

Note that in the case of the ordinary wave mixing the coupling constants have the form $h^{o}_{mn} = a_{\perp}\Delta k_{mnz}\left(\mathbf{e}^{o}_{m\perp}\mathbf{e}^{o}_{n\perp}\right)$.

The detailed analysis of the system of reduced equations describing the FWM shows that the parametric amplification with saturation of only one wave $\mathbf{E}_1$ occurs while three other waves $\mathbf{E}_{2,3,4}$ undergo total depletion [45]

$$z \to \infty,\ W_1 \to 1, W_{2,3,4} \to 0 \quad (90)$$

where

$$W_m = \frac{l_m}{I_0}\left(\frac{\omega}{c}\right)^{-2}\left|A_m\right|^2;\ I_0 = \sum_{m=1}^{4} l_m\left(\frac{\omega}{c}\right)^{-2}\left|A_m\right|^2 = const. \quad (91)$$

The waves with the intensities $W_{2,3}$ and the intermediate frequencies $\omega_{2,3}$ form the spatially localized soliton-like states, if the pumping wave $\mathbf{E}_4$ is strong enough at the input $z = 0$. In the excitation interval $0 < z < \min\left(z_{02}, z_{03}\right)$ three waves $\mathbf{E}_{1,2,3}$ are amplified where z_{02}, z_{03} are the coordinates of the points of maximum for $W_{2,3}$. The intensities $W_{1,2,3,4}$ are non-periodical and stable with respect to the sample thickness and a pumping intensity [45]. Consider the behavior of the phases γ_m. If for all m, n $\left(\Delta\omega_{mn}\right)^2 > \Omega^2_{mn}$, then all phase shifts are negative and the medium is defocusing [48]. In the opposite case $\left(\Delta\omega_{mn}\right)^2 < \Omega^2_{mn}$ the medium is a focusing one [48].

Consider the important case when the pumping wave $\mathbf{E}_4$ and the signal wave $\mathbf{E}_1$ are much stronger than the idler waves $\mathbf{E}_{2,3}$: $W_{1,4} \gg W_{2,3}$. Then the chain of equations similar to the previous section can be obtained, and the solution up to the second approximation has the form [45].

$$W_{10,40} = \frac{J_1}{2}\left[1 \pm \tanh\left[\frac{\beta_{41}J_1}{2}\left(z - z_1\right)\right]\right] \quad (92)$$

$$W_{2,3} = W_{2,3}\left(0\right)\exp\left(a_{1,2}\eta\right)\left[\frac{\cosh\left(\eta_1\right)}{\cosh\left(\eta - \eta_1\right)}\right]^{c_{1,2}} \quad (93)$$

$$W_{11}=\frac{1}{\beta_{41}\left[\cosh\left(\eta-\eta_1\right)\right]^2}\int\limits_0^{\eta}\left[\cosh\left(\eta'-\eta_1\right)\right]^2\left[1+\tanh\left(\eta'-\eta_1\right)\right]\times$$

$$\times\left[\beta_{41}J_2+W_2\left(\beta_{21}-\beta_{41}\right)+W_3\left(\beta_{31}-\beta_{41}\right)\right]d\eta' \tag{94}$$

$$W_{41}=-\frac{1}{\beta_{41}\left[\cosh\left(\eta-\eta_1\right)\right]^2}\int\limits_0^{\eta}\left[\cosh\left(\eta'-\eta_1\right)\right]^2\left[1-\tanh\left(\eta'-\eta_1\right)\right]\times$$

$$\times\left[\beta_{41}J_2+W_2\left(\beta_{42}-\beta_{41}\right)+\varepsilon W_3\left(\beta_{43}-\beta_{41}\right)\right]d\eta' \tag{95}$$

where $W_{1,4}=W_{10,40}+W_{11,41}+...,W_{10,40}\gg\left|W_{11,41}\right|,J_1=W_1\left(0\right)+W_4\left(0\right),$ $J_2=W_2+W_3+W_{11}+W_{41}=const,$

$$\eta=\frac{\beta_{41}J_1z}{2},\ z_1=\frac{1}{\beta_{41}J_1}\ln\left[\frac{W_4\left(0\right)}{W_1\left(0\right)}\right] \tag{96}$$

$$a_1=\frac{\beta_{42}-\beta_{21}}{\beta_{41}},\ a_2=\frac{\beta_{43}-\beta_{31}}{\beta_{41}},\ c_1=\frac{\beta_{42}+\beta_{21}}{\beta_{41}},\ c_2=\frac{\beta_{43}+\beta_{31}}{\beta_{41}} \tag{97}$$

$$\beta_{mn}=\frac{\omega_m^2\omega_n^2I_0\left(h_{mn}^e\right)^2\Delta\omega_{mn}\Gamma_{mn}\left(\Delta k_{mn\perp}\right)^2}{4\pi\rho c^4l_ml_n\left|G_{mn}\right|^2\left(\Delta k_{mn}\right)^2}. \tag{98}$$

The quantities β_{mn} play a role of gain coefficients, and their magnitudes reach maximal values in the resonance case $\left(\Delta\omega_{mn}\right)^2=\Omega_{mn}^2$. Then we obtain

$$\left|\beta_{mn}^{res}\right|=\frac{\omega_m^2\omega_n^2I_0\left(h_{mn}^e\right)^2\left|\Omega_{mn}\right|}{4\pi Bc^4l_ml_n\Gamma_{mn}\left(\Delta k_{mnz}\right)^2}\sim\frac{\omega_mP\varepsilon_a^2\left|\Omega_{mn}\right|}{Bc^2\Gamma_{mn}\sqrt{\varepsilon_{\parallel}\varepsilon_{\perp}}}. \tag{99}$$

Consider expressions (93). It is easy to see that $W_{2,3}\to0$ as $\eta\to\infty$ since $a_1<c_1$ and $a_2<c_2$. The analysis shows [45] that $W_{2,3}$ reach their maxima at the points $z_{02,03}$, determined by

$$z_{02}=\frac{1}{\beta_{41}J_1}\ln\left[\frac{\beta_{42}W_4\left(0\right)}{\beta_{21}W_1\left(0\right)}\right],\ z_{03}=\frac{1}{\beta_{41}J_1}\ln\left[\frac{\beta_{43}W_4\left(0\right)}{\beta_{31}W_1\left(0\right)}\right] \tag{100}$$

that exist if $\beta_{42}W_4\left(0\right)>\beta_{21}W_1\left(0\right)$ and $\beta_{43}W_4\left(0\right)>\beta_{31}W_1\left(0\right)$.

The phases $\gamma_m\left(z\right)$ have the form [45]

$$\gamma_1=-\frac{\delta_{14}}{2\beta_{41}}\ln\left[\frac{\cosh\left(\eta_1\right)\exp\left(\eta\right)}{\cosh\left(\eta-\eta_1\right)}\right], \tag{101}$$

$$\gamma_2=-\frac{1}{2}\ln\left[\exp\left(\frac{\delta_{21}+\delta_{24}}{\beta_{41}}\eta\right)\left(\frac{\cosh\left(\eta-\eta_1\right)}{\cosh\left(\eta_1\right)}\right)^{\mu_1}\right] \tag{102}$$

$$\gamma_3 = -\frac{1}{2}\ln\left[\exp\left(\frac{\delta_{31}+\delta_{34}}{\beta_{41}}\eta\right)\left(\frac{\cosh\left(\eta-\eta_1\right)}{\cosh\left(\eta_1\right)}\right)^{\mu_2}\right], \tag{103}$$

$$\gamma_4 = -\frac{\delta_{14}}{2\beta_{41}}\ln\left[\frac{\exp\left(\eta\right)\cosh\left(\eta-\eta_1\right)}{\cosh\left(\eta_1\right)}\right] \tag{104}$$

where

$$\delta_{mn} = \frac{\omega_m^2\omega_n^2 I_0\left(h_{mn}^e\right)^2\Delta\omega_{mn}\left(\Delta k_{mn\perp}\right)^2\left[\left(\Delta\omega_{mn}\right)^2-\Omega_{mn}^2\right]}{4\pi\rho c^4 l_m l_n\left|G_{mn}\right|^2\left(\Delta k_{mn}\right)^2} \tag{105}$$

and $\mu_1 = \left(\delta_{21}-\delta_{24}\right)/\beta_{41}$, $\mu_2 = \left(\delta_{31}-\delta_{34}\right)/\beta_{41}$. Expressions (101)-(104) show that the depletion of the waves $\mathbf{E}_{2,3,4}$ is accompanied by the cross phase modulation with the infinitely increasing phases while the signal wave phase γ_1 saturates at large distances:

$$\eta\to\infty,\ \gamma_1\to-\frac{\delta_{14}}{2\beta_{41}}\ln\left(1+\frac{W_4\left(0\right)}{W_1\left(0\right)}\right). \tag{106}$$

The so-called polarization-decoupled FWM [65] is possible in SA when some light waves have perpendicular polarizations. Such waves do not excite the dynamic grating (85) since the corresponding coupling constants vanish. For example, let each light wave to be polarized normal to its incidence plane and propagates as an ordinary one. Then the situation is possible when one field is perpendicular to the three others, and as a result, one wave propagates through the nonlinear SA without any change. If $\mathbf{E}_1\perp\mathbf{E}_{2,3}$ and $\mathbf{E}_1\parallel\mathbf{E}_4$, then two independent processes of the nonlinear two wave mixing occur. The solution in such a case represents two pairs of spatial kinks (92) with the different crossing points and excitation lengths [45].

In the particular case when the fundamental waves (81) counterpropagate, an analog of Brillouin enhanced FWM (BEFWM) with a phase conjugation [66] is possible. For the sake of definiteness, assume that the wave $\mathbf{E}_1$ is phase-conjugate with respect to the wave $\mathbf{E}_4$ while the waves $\mathbf{E}_{2,3}$ are forward-going and backward-going pumping waves, respectively. They have the form

$$\mathbf{E}_1 = \mathbf{e}_1\left[A_1\exp i\left(\mathbf{k}_4\mathbf{r}+\boldsymbol{\omega}_1 t\right)+c.c.\right], \tag{107}$$

$$\mathbf{E}_2 = \mathbf{e}_2\left[A_2\exp i\left(\mathbf{k}_2\mathbf{r}-\boldsymbol{\omega}_2 t\right)+c.c.\right] \tag{108}$$

$$\mathbf{E}_3 = \mathbf{e}_3\left[A_3\exp i\left(\mathbf{k}_2\mathbf{r}+\boldsymbol{\omega}_3 t+\Delta\mathbf{k}_f\mathbf{r}\right)+c.c.\right], \tag{109}$$

$$\mathbf{E}_4 = \mathbf{e}_4\left[A_4\exp i\left(\mathbf{k}_4\mathbf{r}-\boldsymbol{\omega}_4 t\right)+c.c.\right] \tag{110}$$

where $\Delta\mathbf{k}_f$ is the wave vector mismatch of FWM process. The frequency balance between the coupled harmonics with the same wave vectors is a

necessary condition for the phase conjugation by stimulated scattering [66]: $\Delta\omega_{31} = \Delta\omega_{42}$. Assuming that the pumping waves $\mathbf{E}_{2,3}$ are strong compared with the probe wave $\mathbf{E}_4$ and the phase-conjugate wave $\mathbf{E}_1$ and using the constant pumping approximation [48], we seek the solution in the form

$$A_{1,4} \sim \exp\left[gr \pm i\frac{(\Delta\mathbf{k}_f\mathbf{r})}{2}\right]. \tag{111}$$

Analysis of the linearized system of the reduced equations for $A_{1,4}$ shows that there exists the root g_1 with the negative real part $\mathrm{Re}\, g_1 < 0$ which corresponds to the amplification of the phase-conjugate wave $\mathbf{E}_1$ propagated in the negative direction [45]. The strong amplification of the phase-conjugate wave $\mathbf{E}_1$ would occur under the condition [45]

$$\frac{\varepsilon_a^2 |A_3|^2 \Omega^-}{8\pi\Gamma^-\sqrt{\varepsilon_\parallel\varepsilon_\perp}} \gg \frac{s_0}{c} \tag{112}$$

where $\Omega^- = \Omega(\mathbf{k}^-) = \Delta\omega_{31}$, $\Gamma^- = \Gamma^-(\mathbf{k}^-), \mathbf{k}^- = \mathbf{k}_4 - \mathbf{k}_2$. Condition (112) can be satisfied for the typical values of the material parameters [1, 2] when the pumping intensity $\sim 100\mathrm{MWcm}^{-2}$ which is feasible [38]. The gain coefficient $|\mathrm{Re}\, g_1|$ is given by [45]

$$|\mathrm{Re}\, g_1| = \frac{h_{42}^2\Omega^- I^+}{8\pi Bl\Gamma^-\left(k_z^-\right)^2} \tag{113}$$

where $l = k_4\left[1 - (\mathbf{k}_4\mathbf{e}_1)\, k_4^{-2}\right]$ and

$$I^+ = \left(\frac{\boldsymbol{\omega}_4}{c}\right)^2 |A_2|^2 + \left(\frac{\omega_1}{c}\right)^2 |A_3|^2. \tag{114}$$

The phase-matched components of the nonlinear polarization perpendicular to the electric field of the fundamental light waves generate their additional components due to the combined effects of nonlinearity and anisotropy. The fundamental waves (81) polarized in the incidence plane generate the additional transverse components with the unit polarization vectors $\mathbf{e}'_{m\perp} = [\mathbf{s}_m \times \mathbf{e}_m]/s_m$ where $\mathbf{s}_m \perp \mathbf{e}_m$ is the beam vector of the extraordinary wave $\mathbf{E}_m$. The additional components have the form [45]

$$E'_{m\perp} = \frac{\omega_m^2}{s_m c^2 k_m^2}\left(\mathbf{D}_m^{NL} \cdot [\mathbf{s}_m \times \mathbf{e}_m]\right). \tag{115}$$

The fundamental waves (81) polarized in the layer plane and perpendicular to the propagation direction cause the longitudinal component of the

nonlinear induction D_{mz}^{NL} given by

$$D_{mz}^{NL} = -\left(\sum_n \frac{a_\perp \left(\mathbf{e}_{m\perp}\mathbf{e}_{n\perp}\right)\Omega_{mn}^2 \left(\Delta\mathbf{k}_{mn\perp}\mathbf{e}_{n\perp}\right)}{4\pi B G_{mn}\Delta k_{mnz}} |A_n|^2\right) \times$$

$$\times \varepsilon_a A_m \exp i\left(\mathbf{k}_m\mathbf{r} - \boldsymbol{\omega}_m t\right) + c.c. \tag{116}$$

which, in turn, generate both transverse and longitudinal field components

$$E'_{mz} = \frac{k_{m\perp}^2}{\left(\varepsilon_\perp k_{m\perp}^2 + \varepsilon_\parallel k_{mz}^2\right)} D_{mz}^{NL},\ E'_{m\perp} = -\frac{k_{mz}\left(\varepsilon_\parallel k_m^2 + \varepsilon_\perp k_{m\perp}^2\right)}{\varepsilon_\perp k_{m\perp}\left(\varepsilon_\perp k_{m\perp}^2 + \varepsilon_\parallel k_{mz}^2\right)} D_{mz}^{NL}. \tag{117}$$

Evidently, the additional components $\mathbf{E}'_m$ are finite and spatially localized [45]: $z \to \infty, E'_m \to 0$.

The components of nonlinear electric induction (36) that are not phase-matched to the fundamental waves (81) give rise to the number of Stokes and anti-Stokes harmonics $\mathbf{f}_l^S = \mathbf{F}_l^S \exp i\psi_l$ with the amplitudes

$$F_l^S \sim \frac{\varepsilon_a^2 |A_m A_n A_p| \Omega_{mn}^2}{4\pi B |G_{mn}|},\ z \to \infty, \left|F_l^S\right| \to 0. \tag{118}$$

The total number of scattered Stokes and anti-Stokes harmonics is equal to 24. The multiplication of 6 harmonics of the dynamic grating (85) and 4 fundamental waves (81) yields 48 terms including 12 phase-matched to the fundamental waves terms. The remaining 36 terms include 12 doubly degenerate terms of the type $A_m A_p A_n^* \exp i\left[\left(\mathbf{k}_m + \mathbf{k}_p - \mathbf{k}_n\right)\mathbf{r} - \left(\omega_m + \omega_p - \omega_n\right)t\right]$ and 12 terms of the type $A_m^2 A_n^* \exp i\left[2\left(\mathbf{k}_m\mathbf{r} - \omega_m t\right) - \left(\mathbf{k}_n\mathbf{r} - \boldsymbol{\omega}_n t\right)\right]$.

5 Light-induced electrodynamic and hydrodynamic excitations in SA

5.1 Light-induced high-frequency longitudinal electric field

LC consist of strongly anisotropic molecules with a large electric dipole moment μ_e. Bend deformations of such molecules cause macroscopic electric polarization. The external electric field creates the bend deformations of molecules. This is the so-called flexoelectric effect, and the deformation induced polarization $\mathbf{P}_f$ is called the flexoelectric polarization [1, 2, 67]. The flexoelectric polarization, in turn, creates a space charge [1]. The additional terms in the LC free energy density caused by the flexoelectric polarization are linear on the external electric field [1] which is equivalent to the breaking

of the inversion symmetry. In NLC the flexoelectric polarization $\mathbf{P}_f$ determined by the bend deformations is described by the director deviations from the equilibrium state. It has the form [1]

$$\mathbf{P}_f = e_1^f \mathbf{n}\,(\mathrm{div}\mathbf{n}) + e_3^f\,[(\mathrm{curl}\mathbf{n}) \times \mathbf{n}] \tag{119}$$

where $e_{1,3}^f \sim \mu_e/a$ are the flexoelectric coefficients. Here a is a characteristic molecular dimension. The flexoelectric coefficients $e_i^f \sim 10^{-11}$C/m [21]. Unlike NLC, the flexoelectric polarization $\mathbf{P}_f$ in SA caused by the layer normal displacement is given by [6]

$$P_{fx} = -e_3^f \frac{\partial^2 u}{\partial z \partial x};\; P_{fy} = -e_3^f \frac{\partial^2 u}{\partial z \partial y};\; P_{fz} = -e_1^f \nabla_\perp^2 u - e_2^f \frac{\partial^2 u}{\partial z^2}. \tag{120}$$

In the static case it is negligibly small as compared to NLC because of a large value of the elastic constant B [6]. However, in the case of the light-induced dynamic grating (85), in the resonance case the flexoelectric polarization may be considerable [47]. The polarization (120) gives rise to the electric field $\mathbf{E}_f$ due to the condition [55] $\mathrm{div}\mathbf{D} = 0$ where

$$D_x = \varepsilon_\perp E_{fx} + 4\pi P_{fx};\; D_y = \varepsilon_\perp E_{fy} + 4\pi P_{fy};\; D_z = \varepsilon_\parallel E_{fz} + 4\pi P_{fz}. \tag{121}$$

Using the Maxwell equations [55] it can be shown that the magnetic field $\mathbf{H}^f$ related to the time dependent flexoelectric polarization (120) can be neglected. Indeed,

$$H_f \sim \frac{1}{c}\frac{\Delta\omega}{\Delta k} P_f \sim \frac{s_0}{c}\frac{k_m}{\Delta k_{mn}} P_f \ll P_f. \tag{122}$$

Hence the high frequency flexoelectric field $\mathbf{E}_f$ is longitudinal and $\mathrm{curl}\mathbf{E}_f = 0$. This condition along with equations (85), (86), (120), and (121) yields [45]

$$\mathbf{E}_f = -\frac{i}{B}\sum_{m,n} \Delta\mathbf{k}_{mn} \frac{h_{mn}\Omega_{mn}^2 \left[\left(e_1^f + e_3^f\right)(\Delta k_{mn\perp})^2 + e_2^f\,(\Delta k_{mnz})^2\right]}{\Delta k_{mnz} G_{mn}\left[\varepsilon_\perp\,(\Delta k_{mn\perp})^2 + \varepsilon_\parallel\,(\Delta k_{mnz})^2\right]} \times$$

$$\times A_m A_n^* \exp i\,(\Delta\mathbf{k}_{mn}\mathbf{r} - \Delta\boldsymbol{\omega}_{mn} t)\,. \tag{123}$$

The flexoelectric field $\mathbf{E}_f$ (123) is spatially localized due to the spatial localization of the light wave amplitudes A_m, A_n^* [45]: $z \to \infty$, $|E_f| \to 0$. At the interface $z = 0$ the field $\mathbf{E}_f$ behaves as a high frequency spatially periodic surface wave. The tangential component of each harmonic (123) wave vector

is continuous at the boundary [55], and for this reason the wave vector $\mathbf{k}_{mn}^{L}$ in a linear medium $z<0$ has a tangential component $\mathbf{k}_{mn\perp}^{L}=\Delta\mathbf{k}_{mn\perp}$. The normal component k_{mnz}^{L} is purely imaginary since

$$k_{mn}^{L}=\frac{\Delta\omega_{mn}}{c}\sim\frac{k_{m}s_{0}}{c}\ll\Delta k_{mn\perp}\sim k_{m}\sin\left(\frac{\Delta\theta}{2}\right) \tag{124}$$

and

$$\left(k_{mnz}^{L}\right)^{2}=\left(k_{mn}^{L}\right)^{2}-\left(\Delta k_{mn\perp}\right)^{2}<0 \tag{125}$$

where $\Delta\theta$ is the angle between the wave vectors of two light waves.

The second harmonic generation (SHG) [48] in NLC and SA is impossible in general case due to their inversion symmetry [21]. However, it has been observed in some special cases when the inversion symmetry is broken due to the external electric or optical fields, boundary effects, light-induced spatial dispersion, etc. [21]. Consider, for example, NLC placed in the external electrostatic field $\mathbf{E}_{0}\parallel\mathbf{n}$. Let the pumping wave $\mathbf{E}\left(\omega\right)$ propagation direction perpendicular to the director $\mathbf{k}\perp\mathbf{n}$. Then the nonlinear polarization with the double frequency $\mathbf{P}_{o,e}^{N}\left(2\omega\right)$ for the ordinary and extraordinary pumping waves $\mathbf{E}^{o}\left(\omega\right),\mathbf{E}^{e}\left(\omega\right)$, respectively has the form [21]

$$\mathbf{P}_{o}^{N}\left(2\omega\right)=\chi_{zxxz}^{(3)}E_{0}\left(E^{o}\left(\omega\right)\right)^{2}\mathbf{n};\ \mathbf{P}_{e}^{N}\left(2\omega\right)=\chi_{zzzz}^{(3)}E_{0}\left(E^{e}\left(\omega\right)\right)^{2}\mathbf{n}. \tag{126}$$

The static flexoelectric polarization $\mathbf{P}_{f}$ (119) also gives rise the nonlinear polarization $\mathbf{P}^{N}\left(2\omega\right)$ which has the form [21]

$$P_{i}^{N}\left(2\omega\right)\sim\chi_{ijkl}E_{i}\left(\omega\right)E_{k}\left(\omega\right)P_{fl}=\chi_{ikl}^{eff}E_{i}\left(\omega\right)E_{k}\left(\omega\right) \tag{127}$$

where the effective nonlinear susceptibility $\chi_{ikl}^{eff}=\chi_{ijkl}P_{fl}$ can be introduced.

A similar effect can occur in SA. However, this time it is related to the light-induced smectic layer deformations and the high-frequency flexoelectric polarization (120). The light-induced electric field $\mathbf{E}_{f}$ (123) breaks the inversion symmetry of SA due to the molecule deformation and permits SHG due to the mixing of the high frequency waves (123) and the fundamental waves on the cubic susceptibility of an electronic origin χ_{ijkl}^{el}. The second harmonic polarization in such a case has the form

$$P_{i}^{NL}\left(2\omega_{m}\right)\sim\chi_{ijkl}^{el}\left(\omega=\omega_{m}+\omega_{n}+\Delta\omega_{mn}\right)E_{fj}\left(\Delta\omega_{mn}\right)E_{mk}\left(\omega_{m}\right)E_{nj}\left(\omega_{n}\right) \tag{128}$$

where the effective quadratic susceptibility

$$\chi_{ikl}^{eff}\sim\chi_{ijkl}^{el}\left(\omega=\omega_{m}+\omega_{n}+\Delta\omega_{mn}\right)E_{fj}\left(\Delta\omega_{mn}\right) \tag{129}$$

Substituting expressions (81) and (123) into (128), we obtain the nonlinear polarization which generates the second harmonic.

$$P_i^{NL}(2\omega_m) \sim -\frac{i}{B}\chi_{ijkl}^{el}(2\omega_m)\frac{h_{mn}\Omega_{mn}^2\left[\left(e_1^f+e_3^f\right)(\Delta k_{mn\perp})^2+e_2^f(\Delta k_{mnz})^2\right]}{\Delta k_{mnz}G_{mn}\left[\varepsilon_\perp(\Delta k_{mn\perp})^2+\varepsilon_\parallel(\Delta k_{mnz})^2\right]}\times$$

$$\times|A_n|^2 A_m^2 \exp i\left(2\mathbf{k}_m\mathbf{r}-2\omega_m t\right). \tag{130}$$

The surface anchoring may be neglected for sufficiently thick monodomain layers of SA ($d \gtrsim 100\mu m$). The specific surface effects such as the surface SHG [21] are not considered in this work.

5.2 Light-induced hydrodynamic flow in SA

In SA any time dependent-normal deformation of the layer results in the hydrodynamic flow according to equations (1) and (6). The normal component v_z of the hydrodynamic velocity is given by (6). Using expressions (85) and (86), we obtain

$$v_z = \sum_{m,n}\frac{\Delta\omega_{mn}h_{mn}^e(\Delta k_{mn\perp})^2}{4\pi\rho G_{mn}(\Delta k_{mn})^2}A_m A_n^* \exp i\left(\Delta\mathbf{k}_{mn}\mathbf{r}-\Delta\omega_{mn}t\right) =$$

$$= \sum_{m,n} V_{mn}\exp i\left(\Delta\mathbf{k}_{mn}\mathbf{r}-\Delta\omega_{mn}t\right). \tag{131}$$

The hydrodynamic flow (131) is a complicated spatiotemporal pattern [61] representing a superposition of 6 harmonics with different spatial periods $\sim(\Delta k_{mn})^{-1}$ and temporal periods $\sim(\Delta\omega_{mn})^{-1}$. For a small difference in frequencies and propagation directions of the fundamental light waves, $k_m \sim k_n$, $\Delta k_{mn} \ll k_m$, and $\Delta\mathbf{k}_{mn}$ is approximately normal to the propagation direction of the coupled light waves. Consequently, according to (1) the hydrodynamic velocity $\mathbf{v}$ would be approximately parallel to the wave vector $\mathbf{k}_m$, i.e. almost coincides with the light wave propagation direction. As a result, for the waves propagating in a direction close to the optical Z axis, the hydrodynamic flow occurs perpendicular to the layer plane. In the opposite case the light waves propagating close to the layer plane give rise to the flow almost parallel to the layer plane. Each harmonic in the series (131) can be characterized by two scales. The short scale is defined by the inverse wave vector difference $(\Delta k_{mn})^{-1}$. The large scale is caused by the spatial inhomogeneity of the slowly varying amplitudes A_m and it is of an order of magnitude of the correlation lengths $(\beta_{mn})^{-1}$. Substituting relations (88),

(91) and (98) into (131), we obtain for the hydrodynamic velocity amplitudes [45]

$$|V_{mn}|^2 = \frac{\beta_{mn} I_0 \Delta\omega_{mn} \Omega_{mn}^2}{4\pi B \Gamma_{mn} \left(\Delta k_{mnz}\right)^2} M_{mn} \tag{132}$$

where the factors M_{mn} are given by

$$M_{mn} = W_m W_n = W_m(0) W_n(0) \exp\left[-\int_0^z \left(\sum_j \beta_{mj} W_j + \sum_i \beta_{ni} W_i \right) dz' \right]. \tag{133}$$

The envelope factor M_{mn} (133) determines the large-scale profile of the hydrodynamic flow containing the combination of energetic, temporal and spatial characteristics of the process. The comparison of relationships (90) and (133) shows that all amplitudes V_{mn} are finite and spatially localized: $z \to \infty, |V_{mn}| \to 0$. All hydrodynamic excitations are convective [68]. $|V_{mn}|^2$ may have a maximum $z_{0mn} > 0$ defined by a condition

$$\sum_j \beta_{mj} W_j(z_{0mn}) + \sum_i \beta_{ni} W_i(z_{0mn}) = 0 \tag{134}$$

that exists if there exist the points $z_{02,03} > 0$ and the crossing point z_1 determined by

$$\int_0^{z_1} \left(\sum_j \beta_{j1} W_j + \sum_i \beta_{4i} W_i \right) dz' = \ln\left[\frac{W_4(0)}{W_1(0)} \right] \tag{135}$$

Hence, the envelopes of the velocity harmonics form spatial solitons [69]. In the particular case of BEFWM (92)-(95) the envelopes have the form [45]

$$M_{14} = \frac{J_1^2}{4\left[\cosh(\eta - \eta_1)\right]^2} \gg M_{mn}, m, n \neq 1, 4 \tag{136}$$

$$M_{12,42} = \frac{J_1 W_2(0)}{2} \exp(a_1 \eta) \left[\frac{\cosh(\eta_1)}{\cosh(\eta - \eta_1)} \right]^{c_1} \left[1 \pm \tanh(\eta - \eta_1)\right] \tag{137}$$

$$M_{13,43} = \frac{J_1 W_3(0)}{2} \exp(a_2 \eta) \left[\frac{\cosh(\eta_1)}{\cosh(\eta - \eta_1)} \right]^{c_2} \left[1 \pm \tanh(\eta - \eta_1)\right] \tag{138}$$

$$M_{23} = W_2(0) W_3(0) \exp\left[(a_1 + a_2)\eta\right] \left[\frac{\cosh(\eta_1)}{\cosh(\eta - \eta_1)} \right]^{c_1 + c_2}. \tag{139}$$

The envelope (136) has a maximum at the crossing point η_1. Other envelopes have the following points of maxima

$$\eta_{012} = \eta_1 + \frac{1}{2}\ln\left(\frac{\beta_{42}+\beta_{41}}{\beta_{21}}\right); \eta_{042} = \eta_1 - \frac{1}{2}\ln\left(\frac{\beta_{41}+\beta_{21}}{\beta_{42}}\right); \qquad (140)$$

$$\eta_{013} = \eta_1 + \frac{1}{2}\ln\left(\frac{\beta_{43}+\beta_{41}}{\beta_{31}}\right); \eta_{043} = \eta_1 - \frac{1}{2}\ln\left(\frac{\beta_{41}+\beta_{31}}{\beta_{43}}\right); \qquad (141)$$

$$\eta_{023} = \eta_1 + \frac{1}{2}\ln\left(\frac{\beta_{42}+\beta_{43}}{\beta_{21}+\beta_{31}}\right). \qquad (142)$$

The hydrodynamic flow is divided into large-scale strata with the different temporal and short-scale spatial periodicity. In the case when the constants β_{mn} are strongly different, the maxima points (140)-(142) are well resolved from one another, and the different strata would be distributed in an approximately symmetric way with respect to the largest maximum η_1 of the component M_{14}. In the opposite case when all β_{mn} are approximately equal, the small components with the rapidly oscillating different phases may be neglected compared to the largest component M_{14}, and the hydrodynamic flow has the soliton profile of this component. Numerical estimations show that all $|M_{mn}|$ vanish for $\eta \sim (4 \div 5)$. The hydrodynamic velocity may reach 10cm/s. The minimal thickness necessary for the excitation of the hydrodynamic spatial soliton in a strong optical field is of an order of magnitude of an excitation (correlation) length $L_E \sim 0.02$cm [45]. SA samples with a thickness $\sim (200 \div 300)\,\mu$m are feasible and have been used for the SLS and SS observation [10, 11, 39].

All results obtained are valid for both homeotropically and planary oriented SA. The necessary condition for the effects mentioned above is the oblique incidence of the light waves with respect to the SA optical axis.

It should be noted that in SA with a finite electric conductivity the light-induced hydrodynamic flow affects substantially the electro-convection process. If dc electric field is applied, the electric current in SA consists of the ion fluxes caused by migration, diffusion and convection [49]. The light-induced high frequency hydrodynamic velocity (131) can be larger than a constant migration velocity of ions with a very low mobility $\mu_{ion} \sim 10^{-10}\mathrm{m}^2/\mathrm{Vs}$ in a dc field $E_{dc} \sim \left(10^3 \div 10^4\right)\mathrm{V/cm}$. As a result, ac current would be predominant which enables the formation of high frequency patterns [61].

6 Conclusions

The characteristics of the specific for SA mechanism of optical nonlinearity related to the layer normal displacement $u(\mathbf{r},t)$ combine some advantages of both orientational and electrostrictive mechanisms. They are characterized by a large cubic nonlinearity compared to ordinary liquid Brillouin nonlinearity, a short time response, a weak temperature dependence, a resonant form of a frequency dependence, and a strong dependence on the directions of light wave polarization and propagation.

Considering the typical nonlinear optical effects in SA caused by a specific mechanism based on the layer displacement and SS, we obtained the following results. The ordinary and extra-ordinary light waves undergo a self-focusing and self-trapping due to the light-induced normal deformations of the layers. Numerical estimations show that the nonlinear part of the SA refraction index responsible for the self-focusing is about 10^{-10}esu which is one or two orders of magnitude larger than that for an orientational Kerr effect in isotropic organic liquids. A bright surface guided light wave can occur at the interface between a linear medium and SA. An arbitrarily polarized light wave propagating in a layer plane undergoes a spatial self-modulation and polarization plane change.

The process of a nonlinear wave-mixing in SA is especially interesting. In combines the dependence on both the large cubic nonlinearity and the large SA optical anisotropy. SLS of two arbitrary polarized light waves on SS transforms into a partially FWM due to the splitting of each wave into ordinary and extra-ordinary waves. Four coupled light waves create a dynamic grating of the layer normal displacement $u(\mathbf{r},t)$ and undergo the parametric energy exchange and cross phase modulation due to the scattering on this grating. The strong resonant scattering and SS wave excitation would occur when the frequency difference of the coupled light waves satisfies the SS dispersion relation (11), (57). The two light waves with the lower frequency are amplified, while the two light waves with the larger frequency are depleted forming a macroscopic squeezed state. The gain coefficient is one or two orders of magnitude larger than the one in isotropic organic liquids. The spectrum of scattered waves consists of 20 Stokes, anti-Stokes and fundamental harmonics. The combination of SA anisotropy and nonlinearity gives rise to the additional components of the fundamental light waves. A sufficiently strong incident light wave excites the secondary light wave and the SS wave similarly to the stimulated Brillouin scattering with a threshold light intensity.

The nondegenerate FWM in SA due to the layer displacement nonlin-

earity mechanism results in the amplification of the light wave with the lowest frequency up to a saturation level. The light wave with the highest frequency is depleted monotonically. The two waves with intermediate frequencies form the spatially localized structures. If the input pumping-signal intensity ratio is high enough, a limited spatial interval exists where three light waves with lower frequencies are amplified. In the special case of the counter-propagated waves and frequency balance which is specific for a phase-conjugation process a kind of BEWFM occurs accompanied by the phase-conjugate wave amplification. The scattered harmonics spectrum contains 24 Stokes and anti-Stokes terms. The numerical estimations are in a good accord with the experimental results [38].

The light-induced dynamic grating of layer normal displacement generates a high frequency longitudinal electric field due to the flexoelectric effect. This electric field breaks the SA inversion symmetry and permits SHG. The light induced electric field does not penetrate into free space and behaves as a surface wave outside the SA sample and as a propagated mode inside the sample.

The light-induced dynamic grating of layer normal displacement results in a hydrodynamic flow with an extremely complicated spatiotemporal pattern having two different spatial scales. The short scale is determined by the inverse wave vectors of the dynamic grating. The large scale is characterized by the same excitation (correlation) lengths as the parametric interaction process of the light waves. All hydrodynamic velocity harmonics are spatially localized. The hydrodynamic flow can be either stratified, or it has a soliton form. The light induced hydrodynamic velocity may reach 10cms^{-1}

Appendix A

Derivation of the equation of motion for a layer displacement

We present here the detailed derivation of the equation of motion (10) using the system of equations (1)-(9). We apply the operator curlcurl to both sides of equation (2). Using the well known identity

$$[\nabla \times [\nabla \times \mathbf{v}]] = \nabla (\nabla \cdot \mathbf{v}) - \nabla^2 \mathbf{v} \tag{143}$$

taking into account condition (2) and the identity $[\nabla \times (\nabla \text{II})] \equiv 0$ we obtain

$$-\rho \nabla^2 \frac{\partial \mathbf{v}}{\partial t} = \nabla (\nabla \cdot \mathbf{\Lambda}) - \nabla^2 \mathbf{\Lambda} + \nabla (\nabla \cdot \mathbf{\Lambda}_{vis}) - \nabla^2 \mathbf{\Lambda}_{vis} \tag{144}$$

where the viscous force $(\Lambda_{vis})_i = \partial\sigma'_{ik}/\partial x_i$. We are interested only in the hydrodynamic velocity component v_z since it is related to the layer displacement $u(\mathbf{r},t)$ according to (6) and to the only non-zero generalized force density component Λ_z (3). Neglecting the small orientational term in the free energy density (7) and substituting relations (7)-(9) into (3) we obtain

$$\Lambda_z = B\frac{\partial^2 u}{\partial z^2} - \frac{1}{8\pi}\frac{\partial}{\partial z}\left[a_\perp\left(E_x^2+E_y^2\right)+a_\parallel E_z^2\right] - \frac{1}{4\pi}\left[\frac{\partial}{\partial x}\left(E_xE_z\right)+\frac{\partial}{\partial y}\left(E_yE_z\right)\right] \tag{145}$$

The contribution of the viscous force $\mathbf{\Lambda}_{vis}$.into the equation for v_z is given by

$$\frac{\partial}{\partial z}\left(\nabla\cdot\mathbf{\Lambda}_{vis}\right) - \nabla^2\Lambda_{visz} = \left[-\alpha_1\nabla_\perp^2\frac{\partial^2}{\partial z^2} - \frac{1}{2}\left(\alpha_4+\alpha_{56}\right)\nabla^2\nabla^2\right]v_z \tag{146}$$

where expressions (1), (4) and (5) are taken into account. Separating the z-component of equation (144) and substituting there equations (6), (145) and (146) we immediately get the equation of motion (10).

Appendix B

Solution of the reduced equations for the partially degenerate FWM

In this section we present the detailed solution of the reduced equations for the slowly varying amplitudes (40) in the case of the partially degenerate FWM discussed in Subsection 4.2. Consider the waves (38) and (39). Let the incidence plane of the waves (38) coincides with the XZ plane. Then the ordinary wave $\mathbf{E}_1^o$ is polarized along the Y axis while the extra-ordinary wave $\mathbf{E}_1^e$ is polarized in the XZ plane and has two components. The corresponding polarization vectors are $\mathbf{e}_1^o = (0,1,0)$ and $\mathbf{e}_1^e = (e_{1x}^e, 0, e_{1z}^e)$ where $\left(e_{1x}^e\right)^2 + \left(e_{1z}^e\right)^2 = 1$. In general case, the incidence plane of the pair of waves $\mathbf{E}_2^{o,e}$ (39) cannot be reduced to the XZ plane. Hence we write for the polarization vectors: $\mathbf{e}_2^o = \left(e_{2x}^o, e_{2y}^o, 0\right)$, $\mathbf{e}_2^e = \left(e_{2x}^e, e_{2y}^e, e_{2z}^e\right)$, $|\mathbf{e}_2^{o,e}| = 1$. The wave vectors of the ordinary waves $\mathbf{k}_{1,2}^o$ satisfy the dispersion relation (20), while the wave vectors of the extra-ordinary waves $\mathbf{k}_{1,2}^e$ satisfy the dispersion relation (21). Substituting expressions (38) and (39) and keeping only the terms with the frequency difference $\Delta\omega = \omega_1 - \omega_2 \sim s_0\omega_1/c \ll \omega_1$ we obtain the following expression for the dynamic grating $u(\mathbf{r},t)$

$$u(\mathbf{r},t) = \frac{i}{4\pi\rho}\sum_{j=1}^{4} U_j \exp\left[\left(\Delta\mathbf{k}_j\mathbf{r}\right) - \Delta\omega t\right] + c.c. \tag{147}$$

where

$$U_j = \frac{h_j R_j \left(\Delta k_{j\perp}\right)^2}{\left(\Delta k_j\right)^2 G_j\left(\Delta\omega, \Delta\mathbf{k}_j\right)} \tag{148}$$

$$R_1 = A_1^e \left(A_2^o\right)^*,\ R_2 = A_1^e \left(A_2^e\right)^*,\ R_3 = A_1^o \left(A_2^o\right)^*,\ R_4 = A_1^o \left(A_2^e\right)^* \tag{149}$$

and the quantities $h_j, \Delta\mathbf{k}_j, G_j\left(\Delta\omega, \Delta\mathbf{k}_j\right)$ are defined by relations (49)-(55). Inserting (147) into the expressions for the nonlinear polarization (15), substituting the terms phase matched to the fundamental waves (38) and (39) into the right-hand side of reduced equations (18) for each wave and separating the real and imaginary parts, we obtain the following system of the first order differential equations for the magnitudes $\left|A_{1,2}^{o,e}(z)\right|$ and phases $\gamma_{1,2}^{o,e}$ of slowly varying amplitudes (40).

$$2l_1^{o,e}\frac{\partial\left|A_1^{o,e}(z)\right|}{\partial z} = -\frac{\omega_1^2}{c^2}\left[p_{3,2}\left|A_2^{o,e}(z)\right|^2 + p_{4,1}\left|A_2^{e,o}(z)\right|^2\right]\left|A_1^{o,e}(z)\right| \tag{150}$$

$$2l_2^{o,e}\frac{\partial\left|A_2^{o,e}(z)\right|}{\partial z} = \frac{\omega_2^2}{c^2}\left[p_{3,2}\left|A_1^{o,e}(z)\right|^2 + p_{1,4}\left|A_1^{e,o}(z)\right|^2\right]\left|A_2^{o,e}(z)\right| \tag{151}$$

$$2l_1^{o,e}\frac{\partial\gamma_1^{o,e}}{\partial z} = -\frac{\omega_1^2}{c^2}\left[q_{3,2}\left|A_2^{o,e}(z)\right|^2 + q_{4,1}\left|A_2^{e,o}(z)\right|^2\right] \tag{152}$$

$$2l_2^{o,e}\frac{\partial\gamma_2^{o,e}}{\partial z} = -\frac{\omega_2^2}{c^2}\left[q_{3,2}\left|A_1^{o,e}(z)\right|^2 + q_{1,4}\left|A_1^{e,o}(z)\right|^2\right] \tag{153}$$

where

$$p_j = \frac{\Delta\omega h_j^2 \left(\Delta k_{j\perp}\right)^2 \Gamma_j}{4\pi\rho\left(\Delta k_j\right)^2 \left|G_j\left(\Delta\omega, \Delta\mathbf{k}_j\right)\right|^2},\ q_j = \frac{h_j^2 \left(\Delta k_{j\perp}\right)^2 \left[\left(\Delta\omega\right)^2 - \Omega_j^2\right]}{4\pi\rho\left(\Delta k_j\right)^2 \left|G_j\left(\Delta\omega, \Delta\mathbf{k}_j\right)\right|^2}$$

We multiply equations (150) by $\left|A_1^{o,e}(z)\right|\omega_1^{-2}c^2$, and equations (151) by $\left|A_2^{o,e}(z)\right|\omega_2^{-2}c^2$ and add the resulting equations which gives the integral of motion of the system (43). It defines the conservation of photon number in the parametric energy exchange between the fundamental waves (38), (39), or the Manley-Row condition [48, 55]. Introducing the dimensionless variables $W_{1,2}^{o,e}$ (42) we replace the integral of motion (43) with relation (41) and rewrite equations (150)-(153) as follows.

$$-\frac{\partial W_1^{o,e}}{\partial z} = \left(\beta_{3,2}W_2^{o,e} + \beta_{4,1}W_2^{e,o}\right)W_1^{o,e},\ \frac{\partial W_2^{o,e}}{\partial z} = \left(\beta_{3,2}W_1^{o,e} + \beta_{1,4}W_1^{e,o}\right)W_2^{o,e} \tag{154}$$

$$\frac{\partial\gamma_1^{o,e}}{\partial z} = -\frac{1}{2}\left[\delta_{3,2}W_2^{o,e} + \delta_{4,1}W_2^{e,o}\right],\ \frac{\partial\gamma_2^{o,e}}{\partial z} = -\frac{1}{2}\left[\delta_{3,2}W_1^{o,e} + \delta_{1,4}W_1^{e,o}\right] \tag{155}$$

where the quantities β_j, δ_j are determined by expressions (48). Equations (154), (155) have the implicit solution (44)-(47). In general case, the analytical solution in a closed form of equations (154), (155) is hardly possible. However, the asymptotic behavior of the solutions (44)-(47) can be studied qualitatively. First of all, the conservation law (41) shows that all intensities $W_{1,2}^{o,e}$ are finite. For $\omega_1 > \omega_2$ the frequency difference $\Delta\omega > 0$, consequently all $\beta_j > 0$ and the integrands in the exponents of expressions (44), (45) are positive definite. Hence $W_1^{o,e} \to 0$ as $z \to \infty$, while the integrals in the exponents of (45) have a finite value, and $W_2^o + W_2^e \to 1$ as $z \to \infty$. Equations (155) describe the cross modulation effect.

Under conditions (58) the expansions (59), (60) are used, and equations (154) can be reduced to the chain of the following coupled equations.

$$\frac{\partial W_{10}^e}{\partial z} = -\beta_1 W_{10}^e W_{20}^o, \ \frac{\partial W_{20}^o}{\partial z} = \beta_1 W_{10}^e W_{20}^o \tag{156}$$

$$\frac{\partial W_1^o}{\partial z} = -\beta_3 W_{20}^o W_1^o, \ \frac{\partial W_2^e}{\partial z} = \beta_2 W_{10}^e W_2^e \tag{157}$$

$$-\frac{\partial W_{11}^e}{\partial z} = \beta_1 \left(W_{20}^o W_{11}^e + W_{10}^e W_{21}^o\right) + \beta_2 W_2^e W_{10}^e \tag{158}$$

$$\frac{\partial W_{21}^o}{\partial z} = \beta_1 \left(W_{20}^o W_{11}^e + W_{10}^e W_{21}^o\right) + \beta_3 W_{20}^o W_1^o \tag{159}$$

Equations (156), (157) yield analytical solutions in a closed form (61), (62) and the rapidly converging solutions in the integral form (63), (64). The corresponding phases are evaluated by substituting the first approximation solutions (61) into (46), (47) which yields expressions (72), (73).

The similar approach is used for the solution of the reduced equation in the case of the non-degenerate FWM (Subsection 4.3). The detailed derivations can be found in Ref. [45].

References

[1] P.G. de Gennes and J. Prost, *The Physics of Liquid Crystals* (Clarendon, Oxford, 2nd ed.,1993).

[2] S. Chandrasekhar, *Liquid Crystals* (Cambridge, New York, 2nd ed., 1992).

[3] I.D. Vagner, B.I. Lembrikov and P. Wyder, *Electrodynamics of Magnetoactive Media* (Springer, Berlin, 2003).

[4] E.I. Katz, Sov. Phys. JETP **32**, 1004 (1971).

[5] V.A. Belyakov, *Diffraction Optics of Complex-Structured Periodic Media* (Springer, New York, 1992).

[6] P.G. de Gennes, J. de Physique, Colloque C4, **30**, C4-65 (1969).

[7] Y. Liao, N.A. Clark, and P.S. Pershan, Phys. Rev. Lett. **30**, 639 (1973).

[8] J.C. Bacri, J. de Physique, Colloque C3, **37**, C3-119 (1976).

[9] V.A. Balandin, E.V. Gurovich, A.S. Kashitsyn, S.V. Pasech'nik, A.A. Tabidze, and A.C. Goldberg, Sov. Phys. JETP **71**, 270 (1990).

[10] L. Ricard and J. Prost, J. de Physique, Colloque C3, **40**, C3-83 (1979).

[11] L. Ricard and J. Prost, J. de Physique **42**, 861 (1981).

[12] I.V. Ioffe and B.I. Lembrikov, Sov. Phys. Solid State **22**, 204 (1980).

[13] D.V.G.L.N. Rao and S. Jayaraman, Appl. Phys. Lett. **23**, 539 (1973).

[14] D.V.G.L.N. Rao and S. Jayaraman, Phys. Rev. A **10**, 2457 (1974).

[15] G.K.L. Wong, and Y.R. Shen, Phys. Rev. Lett. **32**, 527 (1974).

[16] Y.R. Shen, Rev. Mod. Phys. **48**, 1 (1976).

[17] R.M. Herman and R.J. Serinko, Phys. Rev. A **19**, 1757 (1979).

[18] B.I. Lembrikov, Sov. Phys. Tech. Phys. **24**, 386 (1979).

[19] B.Ya. Zel'dovich and N.V. Tabiryan, Sov. Phys. JETP Lett. **30**, 478 (1979).

[20] S.M. Arakelyan, G.A. Lyakhov, and Yu.S. Chilingaryan, Sov. Phys. Uspekhi **23**, 245 (1980).

[21] S.M. Arakelyan and Yu.S. Chilingaryan, *Nelineynaya Optika Zhidkih Krystallov* (*Nonlinear Optics of Liquid Crystals*) (Nauka, Moscow, 1984) (in Russian).

[22] B.Ya. Zel'dovich and N.V. Tabiryan, Sov. Phys. Uspekhi **28**, 1059 (1985).

[23] I.C. Khoo, In: *Progress in Optics*, Ed.: E. Wolf, vol. **26**, p. 105 (North Holland, Amsterdam,1988).

[24] I.C. Khoo and S.T. Wu, *Optics and Nonlinear Optics of Liquid Crystals* (World Scientific, Singapore, 1993).

[25] I.C. Khoo, *Liquid Crystals: Physical Properties and Nonlinear Optical Phenomena* (Wiley Interscience, New York, 1994).

[26] I.C. Khoo and N.V. Tabiryan, Phys. Rev. A **41**, 5528 (1990).

[27] I.C. Khoo, IEEE J. Quant. Electr. **32**, 525 (1996).

[28] I.C. Khoo, S. Slussarenko, B.D. Guenther, and M.V. Wood, Opt. Letters **23**, 253 (1998).

[29] I.C. Khoo, M.V. Wood, B.D. Guenther, Min-Yi Shih and P.H. Chen, J. Opt. Soc Am. B **15**, 1533 (1998).

[30] I.C. Khoo, M.V. Wood, M.Y. Shih, and P.H. Chen, Optics Express (Electronics Journal), **4**, 431 (1999).

[31] I.C. Khoo, P.H. Chen, M.V. Wood, and Min-Yi Shih, Chem. Phys. **245**, 517 (1999).

[32] M. Pecciani, A. De Rossi, G. Assanto, A. De Luca, C.P. Umeton, and I.C. Khoo, Appl. Phys. Lett. **77**, 7 (2000).

[33] I.C. Khoo and Y. Liang, Phys. Rev. E **62**, 6722 (2000).

[34] M.Y. Shih, A. Shishido and I.C. Khoo, Opt. Lett. **26**, 1140 (2001).

[35] I.C. Khoo, P.H. Chen, M.Y. Shih, A. Shishido, and S. Slussarenko, Mol. Cryst. Liq. Cryst. **358**, 1 (2001).

[36] A. Schmid, S. Papernov, Zheng-Wu Li, M. Guardalben, and S.D. Jacobs, Mol. Cryst. Liq. Cryst. **207**, 33 (1991).

[37] I.C. Khoo and R. Normandin, J. Appl. Phys. **55**, 1416 (1984).

[38] I.C. Khoo, R.G. Lindquist, R.R. Michael, Jr., and Pei-Yang, IEEE J. Quant. Electr. **23**, 1344 (1987).

[39] I.C. Khoo, R.G. Lindquist, R.R. Michael, R.J. Mansfield, and P. LoPresti, J. Appl. Phys. **69**, 3853 (1991).

[40] B.I. Lembrikov, Sov. Phys. Technical Physics **25**, 1145 (1980).

[41] B.I. Lembrikov, Sov. Phys. Solid State **23**, 715 (1981).

[42] B.I. Lembrikov, Sov. Phys. Technical Physics **27**, 923 (1982).

[43] G.F. Kventsel and B.I. Lembrikov, Liquid Crystals **16**, 159 (1994).

[44] G.F. Kventsel and B.I. Lembrikov, Liquid Crystals **19**, 21 (1995).

[45] G.F. Kventsel and B.I. Lembrikov, Mol. Cryst. Liq. Cryst. **262**, 591 (1995).

[46] G.F. Kventsel and B.I. Lembrikov, Mol. Cryst. Liq. Cryst. **262**, 629 (1995).

[47] G.F. Kventsel and B.I. Lembrikov, Mol. Cryst. Liq. Cryst. **282**, 145 (1996).

[48] Y.R. Shen, *The Principles of Nonlinear Optics* (John Wiley, New York, 1984).

[49] S.W. Morris, J.R. de Bruyn, and A.D. May, Phys. Rev. A **44**, 8146 (1991).

[50] B. Pura, W. Jeda, and A. Zagorski, Acta Physica Polonica A **93**, 465 (1998).

[51] P.C. Martin, O. Parodi, and P.S. Pershan, Phys. Rev. A **6**, 2401 (1972).

[52] M.J. Stephen and J.P. Straley, Rev. Mod. Phys. **46**, 617 (1974).

[53] L.D. Landau and E.M. Lifshitz, *Theory of Elasticity* (Pergamon, Oxford, 3rd ed., 1986).

[54] E.I. Kats, and V.V. Lebedev, *Dynamika Zhidkikh Krystallov* (*Dynamics of Liquid Crystals*) (Nauka, Moscow, 1988) (in Russian).

[55] L.D. Landau and E.M. Lifshitz, *Electrodynamics of Continuous Media* (Pergamon, Oxford, 2nd ed.,1984).

[56] O. Svelto, In: *Progress in Optics*, Ed.: E. Wolf, vol. **12**, p. 3) (North Holland, Amsterdam, 1974).

[57] R.Y. Chiao, E. Garmire, and C.H. Townes, Phys. Rev. Lett. **13**, 479 (1964).

[58] V.E. Zakharov and A.B. Shabat, Sov. Phys. JETP **34**, 62 (1972).

[59] G.P. Agarwal, In: *Contemporary Nonlinear Optics*, Eds.: G.P. Agarwal and R. Boyd, Chap. 2, p. 76 (Academic Press, New York, 1992).

[60] E. Collett, *Polarized Light* (Marcel Dekker, New York, 1993).

[61] M.C. Gross and P.C. Hohenberg, Rev. Mod. Phys. **65**, 851 (1992).

[62] B. Kryzhanovsky and B. Glushko, Phys. Rev. A **45**, 4979 (1992).

[63] V.S. Starunov and I.I. Fabelinskii, Sov. Phys. Uspekhi **12**, 463 (1970).

[64] A. Yariv, *Quantum Electronics* (John Wiley, New York, 2nd ed., 1975).

[65] W.A. Schreder, M.J. Damzen, and M.H.R. Hutchinson, IEEE J. Quant. Electr. **25**, 460 (1989).

[66] R.W. Boyd and G. Grynberg, In: *Contemporary Nonlinear Optics*, Eds.: G.P. Agarwal and R. Boyd, Chap. 3, p. 86) (Academic Press, New York, 1992).

[67] J. Prost and P.S. Pershan, J. Appl. Phys. **47**, 2298 (1976).

[68] E.M. Lifshitz and L.P. Pitaevskii, *Physical Kinetics* (Pergamon, Oxford, 1981).

[69] R.K. Dodd, J.C. Eilbeck, J.D. Gibbon, and H.C. Morris, *Solitons and Nonlinear Wave Equations* (Academic Press, London, 1984).